

Journal of Visualized Experiments

Analysis of cancer cell invasion and anti-metastatic drug screening using hydrogel micro-chamber array (HMCA)-based plates

--Manuscript Draft--

Article Type:	Invited Methods Article - JoVE Produced Video
Manuscript Number:	JoVE58359R3
Full Title:	Analysis of cancer cell invasion and anti-metastatic drug screening using hydrogel micro-chamber array (HMCA)-based plates
Keywords:	3D multicellular objects; spheroid; hydrogel; Micro-chamber; Invasion assay; ECM; Image analysis; Collective invasion; 3D culture model
Corresponding Author:	Mordechai Deutsch Bar-Ilan University Ramat-Gan, ISRAEL
Corresponding Author's Institution:	Bar-Ilan University
Corresponding Author E-Mail:	motti.jsc@gmail.com
Order of Authors:	Ravid-Hermesh Orit Zurgil Naomi Shafran Yana Afrimzon Elena Sobolev Maria Hakuk Yaron Bar-On Eizig Zehavit Mordechai Deutsch
Additional Information:	
Question	Response
Please indicate whether this article will be Standard Access or Open Access.	Standard Access (US\$2,400)
Please indicate the city, state/province, and country where this article will be filmed . Please do not use abbreviations.	The Biophysical Interdisciplinary Jerome Schottenstein Center for the Research and Technology of the Cellome Physics Department, Bld. 214, Bar Ilan University 52900, Ramat Gan, Israel

April 26, 2018

Nandita Singh, Ph.D.
Senior Science Editor

Dear Nandita,

We would like to submit the manuscript entitled: "Analysis of cancer cell invasion and anti-metastatic drug screening using Hydrogel micro-chamber array-based plates" by Ravid-Hermesh Orit, Zurgil Naomi, Shafran Yana, Afrimzon Elena, Sobolev Maria, Hakuk Yaron, Eizig Zehavit and Deutsch Mordechai, for publication in Journal of Visualized Experiments in the category Cancer Research.

The current study deals with the HMCA-based imaging plate for the preparation of 3D multicellular in-vitro models for the research of tumor invasion and anti-metastatic therapy. JoVE's unique multimedia format for this article will simplify the technical details of 3D tumor spheroids preparation, invasion assay procedure and image analysis performance. The video version of the article will greatly contribute to cancer research area.

Author contributions:

Orit Ravid-Hermesh led this study, carried out experimental design and execution of invasion assay and image analysis of HeLa spheroids including manuscript drafting and preparation.

Naomi Zurgil led and supervised this study, including its experimental design, the process of image analysis, evaluation of results and manuscript drafting and preparation.

Yana Shafran led this study and carried out experimental design and execution of collective invasion assay and image analysis of MCF-7 spheroids including drafting the manuscript.

Maria Sobolev was responsible for tissue culture and for design of the HMC array and its production.

Elena Afrimzon contributed to in-HMC generation and culturing of breast cancer spheroids and she participated in drafting the manuscript.

Yaron Hakuk was responsible for Matlab software programs and contributed to image analysis.

Zehavit Eizig was responsible for Matlab software programs and contributed to image analysis.

Mordechai Deutsch supervised this study, designed and coordinated HMC array production and drafted the manuscript.

This manuscript is original, has not been published before and is not currently being considered for publication elsewhere. We confirm that the manuscript has been read and approved by all named authors and that there are no other persons who satisfied the criteria for authorship, but are not listed. We wish to confirm that there are no known conflicts of interest associated with this publication and there has been no significant financial support for this work that could have influenced its outcome.

We would like to suggest the following potential Reviewers:

1. **Orian Shirihai**, M.D., Ph.D. Division of Endocrinology, Department of Medicine, David Geffen School of Medicine at UCLA, Los Angeles, CA, USA.

emails: shirihai@bu.edu, oshirihai@mednet.ucla.edu

2. **Doron Gerber**, Ph.D., Mina and Everard Goodman Faculty of Life Sciences, Bar-Ilan Institute of Nanotechnology and Advanced Materials (BINA). Bar-Ilan university, Israel.
email: doron.gerber@biu.ac.il
3. **Danny Baranes**, Ph.D., The Department of Molecular Biology, Ariel University, Israel.
email: dannyb@ariel.ac.il
4. **Maria Jose Oliveira**, Ph.D., Tumor and Microenvironment Interaction Group Leader, INEB/i3S, institute for Research and Innovation in Health, University of Porto.
email: mariajo@ineb.up.pt
5. **Ilídio J. Correia**, Ph.D., Associate Professor, Faculty of Health Sciences, Universidade da Beira Interior, Covilhã, Portugal.
email: icorreia@ubi.pt
6. **Catarina Brito**, Ph.D., Head, Advanced Cell Models Lab, Animal Cell Technology Unit, Instituto de Biologia Experimental e Tecnológica (iBET) and Instituto de Tecnologia Química e Biológica António Xavier, Universidade NOVA de Lisboa (ITQB NOVA), Portugal.
email: anabrito@itqb.unl.pt

We thank you for your consideration.

Prof. Mordechai Deutsch
The Biophysical Interdisciplinary Jerome Schottenstein Center
for the Research and the Technology of the Cellome,
Physics Department, Bar Ilan University,
Ramat Gan 5290002, Israel
Phone: 972-3-5318349
Fax: 972-3-5342019
e-mail: motti.jsc@gmail.com

TITLE:

Analysis of Cancer Cell Invasion and Anti-Metastatic Drug Screening Using Hydrogel Micro-Chamber Array (HMCA)-Based Plates

AUTHORS & AFFILIATIONS:

Ravid-Hermesh Orit¹, Zurgil Naomi¹, Shafran Yana¹, Afrimzon Elena¹, Sobolev Maria¹, Hakuk Yaron¹, Bar-On Eizig Zehavit¹ and Deutsch Mordechai¹

¹Physics Department, Bar-Ilan University, Ramat-Gan, Israel

Email Addresses:

Ravid-Hermesh Orit (orittravidh@gmail.com)

Zurgil Naomi (zurgiln@gmail.com)

Shafran Yana (yana.shafran@gmail.com)

Afrimzon Elena (elena.afrimzon@biu.ac.il)

Sobolev Maria (eweryday@yahoo.com)

Hakuk Yaron (yaron.hakuk@gmail.com)

Bar-On Eizig Zehavit (zehavit.aizig@gmail.com)

Deutsch Mordechai (motti.jsc@gmail.com)

CORRESPONDING AUTHOR:

Deutsch Mordechai

KEYWORDS:

3D multicellular objects, spheroid, hydrogel, micro-chamber, invasion assay, ECM, image analysis, collective invasion, 3D culture model

SHORT ABSTRACT:

A HMCA-based imaging plate is presented for invasion assay performance. This plate facilitates the formation of three-dimensional (3D) tumor spheroids and the measurement of cancer cell invasion into the extracellular matrix (ECM). The invasion assay quantification is achieved by semi-automatic analysis.

LONG ABSTRACT:

Cancer metastasis is known to cause 90% of cancer lethality. Metastasis is a multistage process which initiates with the penetration/invasion of tumor cells into neighboring tissue. Thus, invasion is a crucial step in metastasis, making the invasion process research and development of anti-metastatic drugs, highly significant. To address this demand, there is a need to develop 3D *in vitro* models which imitate the architecture of solid tumors and their microenvironment most closely to *in vivo* state on one hand, but at the same time be reproducible, robust and suitable for high yield and high content measurements. Currently, most invasion assays lean on sophisticated microfluidic technologies which are adequate for research but not for high volume drug screening. Other assays using plate-based devices with isolated individual spheroids in each well are material consuming and have low sample size per condition. The goal

of the current protocol is to provide a simple and reproducible biomimetic 3D cell-based system for the analysis of invasion capacity in large populations of tumor spheroids. We developed a 3D model for invasion assay based on HMCA imaging plate for the research of tumor invasion and anti-metastatic drug discovery. This device enables the production of numerous uniform spheroids per well (high sample size per condition) surrounded by ECM components, while continuously and simultaneously observing and measuring the spheroids at single-element resolution for medium throughput screening of anti-metastatic drugs. This platform is presented here by the production of HeLa and MCF7 spheroids for exemplifying single cell and collective invasion. We compare the influence of the ECM component hyaluronic acid (HA) on the invasive capacity of collagen surrounding HeLa spheroids. Finally, we introduce Fisetin (invasion inhibitor) to HeLa spheroids and nitric oxide (NO) (invasion activator) to MCF7 spheroids. The results are analyzed by in-house software which enables semi-automatic, simple and fast analysis which facilitates multi-parameter examination.

INTRODUCTION:

Cancer death is attributed mainly to the dissemination of metastatic cells to distant locations. Many efforts in cancer treatment focus on targeting or preventing the formation of metastatic colonies and progression of systemic metastatic disease¹. Cancer cell migration is a crucial step in the tumor metastasis process, thus, the research of the cancer invasion cascade is very important and a prerequisite to finding anti-metastatic therapeutics.

The use of animal models as tools for studying metastatic disease has been found to be very expensive and not always representative of the tumor in humans. Moreover, the extracellular microenvironment topology, mechanics and composition strongly affect cancer cell behavior². Since *in vivo* models inherently lack the ability to separate and control such specific parameters which contribute to cancer invasion and metastasis, there is a need for controllable biomimetic *in vitro* models.

In order to metastasize to distant organs, cancer cells must exhibit migratory and invasive phenotypic traits which can be targeted for therapy. However, since most *in vitro* cancer models do not mimic the actual features of solid tumors³, it is very challenging to detect physiologically relevant phenotypes. In addition, the phenotypic heterogeneity that exists within the tumor, dictates the need for analyzing tumor migration at single-element resolution in order to discover phenotype-directed therapies, for instance, by targeting the metastasis-initiating cell population within heterogeneous tumors⁴.

The study of cell motility and collective migration is primarily conducted in monolayer cultures of epithelial cells on homogeneous planar surfaces. These conventional cellular models for cancer cell migration are based on the population analysis of individual cells invading through the membranes and ECM components⁵, but in such systems, the intrinsic differences between individual cells cannot be studied. Generating 3D spheroids either via scaffolds or in scaffold-free micro-structures is considered as a superior means to study the tumor cell growth and cancer invasion⁶⁻⁸. However, most 3D systems are not suitable to high throughput formats, and

inter-spheroid interaction cannot usually be achieved since isolated individual spheroids are generated in each micro-well⁹. Recent studies involving the cancer migration are based on microfluidic devices^{3,10-12}, however, these sophisticated microfluidic tools are difficult to produce and cannot be used for high throughput screening (HTS) of anti-invasive drugs.

Two main phenotypes, collective and individual cell migration, which play a role in tumor cells overcoming the ECM barrier and invading neighboring tissue, have been demonstrated^{13,14}, each displaying distinct morphological characteristics, biochemical, molecular and genetic mechanisms. In addition, two forms of migrating tumor cells, fibroblast-like and amoeboid, are observed in each phenotype. Since both, invasion phenotypes and migration modes, are mainly defined by morphological properties, there is a need for cellular models that enable imaging-based detection and examination of all forms of tumor invasion and migrating cells.

The overall goal of the current method is to provide a simple and reproducible biomimetic 3D *in vitro* cell-based system for the analysis of invasion capacity in large populations of tumor spheroids. Here, we introduce the HMCA-based 6-well imaging plate for the research of tumor invasion and anti-metastatic therapy. The technology enables the formation of large numbers of uniform 3D tumor spheroids (450 per well) in a hydrogel micro-chambers (MC) structure. Various ECM components are added to the spheroid array to enable the invasion of the cells into the surrounding environment. Invasion process is continuously monitored by short- and long-term observation of the same individual spheroids/invading cells and facilitates morphological characterization, fluorescent staining and retrieval of specific spheroids at any point. Since numerous spheroids share space and medium, interaction via soluble molecules between individual spheroids and their impact on one another is possible. Semi-automatic image analysis is performed by using in-house MATLAB code which enables faster and more efficient collection of large amount of data. The platform facilitates accurate, simultaneous measurement of numerous spheroids/invading cells in a time-efficient manner, allowing medium throughput screening of anti-invasion drugs.

PROTOCOL:

1. HMCA Plate Embossing

Note: The complete process for the design and fabrication of polydimethylsiloxane (PDMS) stamp and HMCA imaging plate used in this protocol is described in detail in our previous articles^{15,16}. The PDMS stamp (negative shape) is used to emboss the HMCA (positive shape) which consists of approximately 450 MCs per well (**Figure 1A**). As demonstrated in **Figure 1B**, each of the MCs has a shape of a truncated upside-down square-shaped pyramid (190 μm - height, 90 μm x 90 μm - small base area and 370 μm x 370 μm - large base area). The HMCA plate is used for the preparation and culturing of 3D tumor spheroids and thereafter, for invasion assay. Alternatively, a commercial stamp could be used for HMCA production.

1.1. Prepare a solution of 6% low melting agarose (LMA). Insert the LMA powder and sterile phosphate buffered saline (PBS) (0.6 g of LMA per 10 mL of PBS) into a glass bottle with a magnetic stirrer. Place the bottle on a heating plate and stir the solution while heating to 80 °C for a few hours until a uniform solution is achieved. Keep the solution at 70 °C until use.

1.2. Pre-heat the PDMS stamp to 70 °C in the oven. Keep it warm until use. Alternatively, use a commercial stamp and follow the instruction.

1.3. Place the commercial 6-well glass-bottom plates on a dry bath pre-heated to 60 °C. Wait a few minutes until the plate is totally warm.

1.4. Pour a drop (400 µL) of pre-heated LMA onto the glass bottom of each one of the wells in the plate. Gently place the pre-heated PDMS stamp over the agarose drop. Incubate at room temperature (RT) for 5-10 min for pre-gelling and pre-cooling. Incubate at 4 °C for 20 min to achieve full agarose gelation. Then, gently peel off the PDMS, leaving the agarose gel patterned with MCs.

Note: This step is done simultaneously in all the wells.

1.5. Place the embossed plate in a light curing system equipped with ultraviolet (UV) lamp, and incubate for 3 min.

Note: Now the HMCA plate is UV sterilized.

1.6. Fill the macro-wells with sterile PBS to ensure that they are kept humid, then cover the plate, wrap it with parafilm and store it at 4 °C until use.

1.7. Before use, empty PBS residuals from the HMCA plate. Place it in the biological hood.

2. Loading Cells and Spheroid Formation

2.1. Collect the cells as follows: remove all medium from a 10 cm culture plate cell monolayer, wash twice with 10 mL of PBS to dispose of serum residuals, add 5 mL of trypsin (pre-warmed to 37 °C) and incubate for 3 min in the incubator at 37 °C. Then, shake the plate gently to ensure monolayer detachment, add 10 mL of complete medium (pre-warmed to 37 °C) and pipette up and down until homogenous cell suspension is achieved. Centrifuge and wash the cell suspension with 15 mL of fresh medium, then, suspend at appropriate concentrations in fresh complete medium.

2.2. Gently load the cell suspension (50 µL, 150×10^3 cells/mL in medium, ~16 cells per MC) on top of the HMCA and allow the cells to settle by gravity for 15 min.

2.3. Gently add 4-8 aliquots of 250 μ L fresh medium (total 2 mL) to the rim of the macro-well plastic bottom outside the ring and hydrogel array.

2.4. Incubate HeLa cells for 72 h and MCF7 cells for 48 h at 37 °C and 5% CO₂ in a humidified atmosphere for the formation of spheroids.

3. Viability Detection by Propidium Iodide (PI) Staining

3.1. Prepare a stock solution of PI (500 μ g of PI per 1 mL of PBS). Keep it at 4 °C for about 6 months. Freshly prepare a dilution of 1:2000 (0.25 μ g/mL), by the addition of 6 μ L of stock to 12 mL of complete medium without phenol red, for the 6-well HMCA plate (2 mL per well).

3.2. Transfer the HMCA plate with 48-72 h spheroids, from the incubator to the biological hood. Remove all medium from the HMCA by leaning the tip end on the edge of the macro-well plastic bottom beside the hydrogel array, leaving the array tank filled with medium.

3.3. Gently add 2 mL of PI dilution from Step 3.1 to each well, by leaning the tip end on the edge of the macro-well plastic bottom. Incubate the HMCA plate for 1 h at 37 °C and 5% CO₂ in a humidified atmosphere. Continue to Step 7.

Note: Other dyes could be used here as well, for example, Hoechst for nucleus staining, tetramethylrhodamine methyl ester (TMRM) for mitochondrial membrane potential staining, fluorescein diacetate (FDA) for live cells detection, Annexin V for apoptosis detection and others.

4. Collagen Mixture Preparation

4.1. Prepare sterile double distilled water (DDW) by autoclave and a stock of 100 mL of 1 M NaOH filter-sterilized solution. Maintain the materials at RT, and the tips used for collagen mixture preparation frozen at -20 °C, until use.

4.2. 10-20 min before use, place all intergrades including: sterile DDW, 1 M NaOH sterile solution, sterile 10x PBS, type I collagen from rat tail (stored at 4 °C for 3-12 months) and a sterile tube into the ice bucket until totally cooled. Place the ice bucket inside the biological hood.

4.3. Prepare 1800 μ L of collagen mixture at a final concentration of 3 mg/mL, for 6-well HMCA invasion assay plate (300 μ L per well) as follows. Add the intergrades into the cooled tube in the following order: 515 μ L of DDW, 24.8 μ L of 1 M NaOH and 180 μ L of 10x PBS. Mix well by vortex and place back into the ice. Finally, add 1080 μ L of collagen to the mixture, vortex again and put back into ice.

5. HA & Collagen Mixture Preparation

214
215 5.1. Dissolve 10 mg of HA in 2 mL of sterile DDW. Incubate the mixture at RT for a few
216 minutes and vortex gently until the powder is totally dissolved. Store the stock solution at 4 °C
217 for up to two years.

218
219 5.2. Right before use, place the HA stock solution in the ice bucket inside the biological
220 hood.

221
222 5.3. Prepare a 3 mg/mL collagen mixture as described in Step 4. Add 36 µg (7.2 µL) of HA
223 into 1800 µL of ready to use collagen mixture, for a final concentration of 20 µg/mL. Then,
224 vortex again briefly and put back into ice.

225 226 **6. ECM Mixture Addition**

227
228 6.1. Transfer the HMCA plate, with 48-72 h spheroids, from the incubator into the biological
229 hood and place it on the ice. Incubate for 10 min until the plate is cooled. Pre-heat a solution of
230 1% LMA to 37 °C in a water bath.

231
232 6.2. Remove all medium from around the HMCA, by leaning the tip end on the edge of the
233 macro-well plastic bottom beside the hydrogel array. Then, very carefully, remove all medium
234 from the array tank with a fine tip/gel loading tip, by leaning the tip end on the array edge,
235 gently and slowly sucking all medium out.

236
237 Note: After removing all medium from around the hydrogel array, the array tank is still filled
238 with medium. This medium has to be removed very gently in order to avoid destruction of the
239 hydrogel MC and dislocation of spheroids.

240
241 6.3. Take 150 µL of the collagen mixture or HA and collagen mixture (ECM mixture) with the
242 pre-frozen fine tip and add into the array tank by attaching the tip to the array edge. Release
243 the mixture slowly to avoid spheroid dislocation. Repeat this step with another aliquot of 150
244 µL, for a total 300 µL per well. Follow the same procedure for each well until all wells are filled.
245 Then place the plate into the incubator for 1 h for the full gelation of the ECM.

246
247 6.4. After the full gelation of ECM has been achieved, pipette 400 µL of pre-warmed 1% LMA
248 on top of the ECM gel. Cover the plate with its lid, incubate the plate at RT for 5-7 min and then
249 for 2 min at 4 °C, for agarose gelation. Finally, gently add 2 mL of complete medium by leaning
250 the tip end on the edge of the macro-well plastic bottom.

251
252 Note: The agarose layer prevents the detachment of the collagen-gel matrix from the HMCA.

253 254 **7. Invasion Assay Acquisition and Analysis**

255

7.1. Load the HMCA plate onto a motorized inverted microscope stage equipped with an incubator, pre-adjusted to 37 °C, 5% CO₂ and humidified atmosphere.

7.2. Pre-determine the positions for image acquisition in each well so as to cover the whole array area, and use 10X or 4X objectives (this step is required for the image acquisition software used here, see the **Materials Table** below for details). Alternatively, use any image acquisition software to facilitate automatic scan of the entire required area, by choosing the **Stich** option.

7.3. Acquire bright field (BF) images every 2-4 h for a total period of 24-72 h in order to follow the invasion of cells from the spheroid body into the surrounding ECM.

7.4. Acquire fluorescent images for PI detection by using a dedicated fluorescent cube (excitation filter 530-550 nm, dichroic mirror 565 nm long pass and emission filter 600-660 nm).

7.5. Export time-lapse BF/fluorescent images from the image acquisition software and save them in tagged image file format (TIFF) to a dedicated folder by using the **Database** tab in the toolbar and then the **Export record files** button.

Note: We developed a special in-house analysis code in MATLAB software that includes a designed graphic user interface (GUI) in which invasion analysis could be executed faster and easier. In this analysis code, the segmentation of the spheroids and invasion area is done semi-automatically using Sobel filter followed by the morphological operators Erosion and Dilation. After automatic segmentation of the areas, manual corrections were made where needed for better accuracy. After the segmentation completion, a set of parameters were automatically calculated by the software and exported to an excel file for further manipulation. The list of parameters are: basic spheroid sectional area at time = 0, invasion area of cells connected to spheroid body = main invasion area, area of cells separated from main invasion area, number of cells separated from main invasion area, average distance of invasion from the basic spheroid center of mass to the circumference of the main invasion area and separated cells and collective invasion distance parameter = d ($d = \sqrt{(X_2 - X_1)^2 + (Y_2 - Y_1)^2}$ out of the X and Y spheroid center of mass coordinates, before (X_1 , Y_1) and after (X_2 , Y_2) collective invasion process). Alternatively, image analysis could be done with any other specialized software.

7.6. Open the GUI and push the **Load BF** button. After the image is open, adjust the segmentation parameters (minimum size: >1 and radius close: >1) to achieve a precise segmentation of spheroid and its invasion area, then, press **Region of interest (ROI) segmentation** button for execution and a border will appear around each spheroid. If the automatic segmentation is incorrect, press the **Delete** or **Add** button and make the requested corrections manually. Repeat the same steps for subsequent images.

7.7. Press the **Tracking** button to number the spheroids and the software will assign the same number for each spheroid in each of the time lapse images. Then, press the

Measurement button, which will generate a spreadsheet with all parameters. Save this spreadsheet as an excel file for further use in results processing and statistics in excel software.

REPRESENTATIVE RESULTS:

The unique HMCA imaging plate is used for the invasion assay of 3D tumor spheroids. The entire assay, beginning with the spheroid formation and ending with the invasion process and additional manipulations, is performed within the same plate. For the spheroid formation, HeLa cells are loaded into the array basin and settle in the hydrogel MCs by gravity. The hydrogel MCs, which have non-adherent/low attachment characteristics, facilitate the cell-cell interaction and the formation of 3D tumor spheroids. **Figure 2A** illustrates the cells settled in the MCs, following the use of 150×10^3 cells/mL loading solution (*i.e.*, ~16 cells per MC calculated value). It is clear that the occupancy of cells per MC is not evenly distributed through the array, and the average obtained statistic distribution is 14.78 ± 3.60 cells per MC. The table in **Figure 2B** summarizes the cell distribution per MC for the whole HMCA plate. The average coefficient of variation (CV) of the cell distribution within a macro-well is 43.33%, while between the macro-wells it is 24.37%. The differences in cell occupancy are crucial and directly dictate the size of spheroids formed and their homogeneity throughout the plate. In order to reduce/minimize the variability created by the number of cells per MC, the analysis of the results is performed at single-element resolution. The plots in **Figure 2C-D** illustrate the size (sectional area) distribution of 3-day spheroids. It is clearly exemplified in **Figure 2D** that calculating the growth ratio of each spheroid (sectional area at day 3/day 2) has a more homogeneous distribution than the absolute size distribution (**Figure 2C**), yielding a CV of 15.48% and 52.80%, respectively. Spheroid diameter distribution of 3-day spheroids yields a CV of 24.52% and the growth ratio (diameter at day3/day2) is 7.45%. These CV values are similar to¹⁷ or higher than¹⁸ other reports attaining cell loading by gravity. In order to eliminate the measured parameter variance resulting from the variability in the initial seeded cell number per MC, it is preferable to normalize the selected parameters to the initial cell number or to any other measured parameter of the same object, such that each spheroid has its internal control. This approach could be easily applied by tracking the object on the HMCA imaging plate.

The process of spheroid formation and growth could be easily followed on the HMCA imaging plate. **Figure 3A-B** shows a BF image of one region on the HMCA imaging plate containing 24-h HeLa cell aggregates and the respective image of mature, 5-day 3D multicellular objects, which are becoming more spherical and denser. It is clearly shown that most objects retain their location during the 5-day incubation period. The analysis of shape (sphericity) and size (sectional area) during the spheroid formation is presented in **Figure 3C**. The scatter plot demonstrates the increases in both parameters from day 1 to day 5; 0.544 ± 0.020 a.u. to 0.684 ± 0.016 a.u. for sphericity ($p < 0.05$) and 0.00356 ± 0.00013 mm² to 0.00538 ± 0.00015 mm² for sectional area ($p < 0.05$), respectively. While 24-h aggregates are small and have non-regular shape, the respective 5-day spheroids are bigger and acquire spherical form.

The detection of spheroid cell viability is executed by using low concentration PI for staining¹⁹ which circumvents the need for dye washing. PI penetrates the cell membrane and then

intercalates into the DNA of non-viable cells. **Figure 4A** shows 5-day HeLa spheroids stained with PI (in red). Analysis of the percentage of red area (representing dead cells) out of each spheroid sectional area is summarized in **Figure 4B**. The histogram shows that 85% of spheroid population has a maximal value of 5% red stained area and the average is 3.01 ± 2.34 % (left histogram). Sectional area of spheroids (right histogram) shows a normal distribution with average of 0.02447 ± 0.00487 mm².

After producing 3-day mature HeLa spheroids, the invasion assay is performed within the HMCA imaging plate. The effect of variables, such as ECM composition, inhibitors and activators, on the 3D tumor spheroid invasion process could be examined. For invasion assay performance, the medium is gently removed and replaced with ECM solution pipette over the spheroids into the MC array basin. After the full gelation of the ECM solution, complete medium is added into the macro-well. (1) In order to examine the influence of HA on the HeLa spheroid spontaneous invasion process, the spheroids were covered with collagen and HA mixture solution (**Figure 5A**) and compared to those covered with collagen only solution (**Figure 5C**), and BF images were acquired right after ECM gelation ($t = 0$ h). The kinetic of invasion process was followed by imaging the same regions every 5 h for a period of 63 h. After 50 h of incubation, the spheroids embedded in collagen and HA (**Figure 5B**) showed lower cell dispersion into the surrounding ECM as compared to the spheroids embedded in collagen only (**Figure 5D**). The analysis of the invasion area kinetic over time, for 99 spheroids at single-spheroid resolution is summarized in **Figure 5E**. **Figure 5E** plots the mean/average invasion area over time of the two groups, and clearly demonstrates that the addition of HA to collagen inhibits the cell dispersion out of the spheroid, resulting in smaller invasion areas. The average of the slopes resulting from linear regression adjustment curves for each of the spheroids embedded in collagen (0.001973 ± 0.000894 mm²/h) as compared to collagen and HA solution (0.001410 ± 0.000941 mm²/h) are significantly different ($p = 0.003$, t-test: two-sample assuming equal variances). (2) In order to examine the influence of Fisetin (a bioactive flavonoid found in several fruits and vegetables which shows cytostatic and migrastatic activities by acting on several molecular targets including phosphatidylinositol 3-kinase (PI3K)/Akt/c-Jun N-terminal kinases (JNK) signaling and Wnt/ β -catenin signaling downregulates matrix metalloproteinases (MMPs) and others²⁰) on HeLa spheroid spontaneous invasion process, increasing concentrations of the drug were added to the complete medium and BF images were acquired at $t = 0$ (**Figure 6A**) and 24 h later (**Figure 6B-C**). As demonstrated, 10 μ M of Fisetin (**Figure 6C**) inhibits the dispersion of cells around the spheroids as compared to non-treated HeLa spheroids (**Figure 6B**). The invasion area analysis of a dose response experiment (**Figure 6D**) exhibits significant inhibition at 10-40 μ M of Fisetin ($p < 0.003$), attaining saturation at the concentration of 10 μ M and higher. (3) It has been shown that NO, at a nano-molar level, contributes to a more aggressive breast cancer phenotype by stimulating tumor expansion and migration¹⁶. In order to examine the influence of NO on the collective invasion process of MCF7 spheroids embedded in collagen, 1 μ M of diethylenetriamine/nitric oxide donor (DETA/NO) was added to the complete culture medium and BF images were acquired at $t = 0$ and $t = 20$ h. Dramatic changes in the morphology and locations of 3D spheroids during exposure to NO donor are evident (**Figure 7A-B**). The spheroids lose their sphericity and become more

elongated acquiring amoeboid migratory phenotype. Concomitantly, enhanced translocation of the spheroids within the surrounding collagen matrix was observed (**Figure 7C**). The average elongation value significantly increased from 1.305 ± 0.193 a.u. to 1.477 ± 0.298 a.u., ($p < 0.0006$). The average migration distance measured for the same spheroids was significantly extended, 0.0788 ± 0.0575 mm and 0.3164 ± 0.3365 mm in the absence and in the presence of DETA/NO, respectively ($p < 4 \times 10^{-6}$).

Image analysis of the spheroid invasion was achieved by semi-automatic in-house MATLAB software. The acquired time lapse images of spheroid formation and invasion within the HMCA consists of numerous spheroids in one image (4-6 spheroids at 10X magnification and 25-30 spheroids at 4X magnification). The analysis of spheroid formation, growth and invasion was concomitantly performed on all spheroids in the image. The key parameters extracted for spheroid invasion are presented in **Figure 8A**, which shows a representative image segmentation of 4 spheroids at a single time point ($t = 16$ h). The main invasion area defined by a red border, as well as the separated cells which disengaged and dispersed around it (indicated by black arrows), were tracked and numbered for each spheroid over time. Spheroid size before invasion at $t = 0$ is defined by a blue border. The mean/average invasion distance from spheroid center of mass to the invasion area circumference including separated cells is calculated from the encircled red segmentation and indicated by yellow arrows. Data extracted from this time-lapse experiment is summarized in **Figure 8B-D**. **Figure 8B** exhibits the elevation of the mean invasion distance from each spheroid center over time. **Figure 8C** exhibits the elevation of the total invasion area in each of the spheroids over time (including the main invasion area and separated/disengaged-cell area). **Figure 8D₁₋₄** shows the magnitude of separated-cell area compared to the total invasion area of each spheroid (over time). The cumulative number of disengaged cells is 33, 7, 4 and 5 for spheroids #1, #2, #3 and #4, respectively. The analysis of cumulative numbers of disengaged cells over 20 h of invasion obtained from 126 HeLa spheroids embedded in collagen is shown in **Figure 8E**. It is demonstrated here that there is a vast distribution in the number of disengaged cells in the examined population and the average value is 12.3 ± 12.8 cells.

FIGURE LEGENDS:

Figure 1: The HMCA imaging plate. (A) Image of one macro-well embossed with HMCA. (B) A cross section of one MC within the HMCA imaging plate.

Figure 2: Homogeneity of the cell distribution and spheroid growth ratio in the HMCA imaging plate. (A) An overlay of BF and fluorescent images of the HMCA loaded with HeLa cells pre-stained with Hoechst 33342 $1 \mu\text{g/mL}$ (loading concentration 150×10^3 cells per mL). Images were acquired right after the cell settlement in the MC. Image magnification 4X, scale bar = $500 \mu\text{m}$. (B) The table summarizes the distribution of HeLa cells within the HMCA-6-well imaging plate. The cells were counted from up to 90 MC/macro-well. The results are presented as mean \pm standard deviation (SD), CV ($\text{SD}/\text{mean} \times 100$) is calculated within and between the macro-wells. (C) Distribution histogram of the sectional area of 3-day spheroids, $n = 418$, determined

from BF images. (D) Distribution histogram of the spheroid growth ratio (sectional area at day 3/day 2). Growth ratio is calculated at single-element resolution for each of the 418 spheroids.

Figure 3: Tracking spheroid formation in the HMCA imaging plate. BF image of HeLa cells (loading concentration 120×10^3 cells per mL) incubated in the HMCA for 1 day (A) and 5 days (B). Image magnification 4X, scale bar = 500 μm . (C) Scatter plot of 3D object sphericity as a function of its sectional area, after 1 day (blue diamonds) and 5 days (brown squares) of incubation post cell loading. Each marker represents the analyzed data from a single spheroid, $n = 83$.

Figure 4: Detection of cell viability in mature spheroids. An overlay of BF and fluorescent images of 5-day spheroids (loading concentration 360×10^3 cells per mL) stained with PI 0.25 $\mu\text{g/mL}$ (A). Image magnification 4X, scale bar = 500 μm . (B) Distribution histogram of the percent of PI area relative to the sectional area of the spheroid (left panel) and distribution histogram of sectional area (right panel), $n = 84$. Percent of PI area is calculated at single-element resolution for each of the 84 spheroids.

Figure 5: Influence of ECM composition on spheroid invasion process. BF images of 3-day HeLa spheroids embedded in a mixture of 3 mg/mL collagen & 20 $\mu\text{g/mL}$ HA (A) and 3 mg/mL collagen (C), at $t = 0$ h and after 50 h of incubation (B) and (D), respectively. Image magnification 10X, scale bar = 200 μm . The HMCA imaging plate was loaded onto the stage of the inverted microscope equipped with incubator. Images were acquired every 5 h and the kinetic analysis is presented in plot (E), $n = 99$. Each curve represents the mean \pm SD of invasion area increase over time, for collagen and HA (blue diamonds) and for collagen only (brown squares). Average linear regression curve and its equation and R-squared value are indicated above the curves.

Figure 6: Fisetin inhibits spontaneous invasion of HeLa spheroids. BF images of 3-day HeLa spheroids, embedded in a mixture of 3 mg/mL collagen (A) at $t = 0$ and then, 24 h after addition of 0 μM (B) and 10 μM Fisetin (C) to the complete culture medium. Image magnification 4X, scale bar = 500 μm . Analysis of invasion area for each spheroid at end point ($t = 24$ h) is presented in plot (D), $n = 488$. The curve represents mean \pm SD of invasion area as a function of 0-40 μM Fisetin. Fisetin treatment significantly inhibits the invasion at 10 μM ($P = 4.65 \times 10^{-6}$), 20 μM ($P = 0.0021$) and 40 μM ($P = 4.86 \times 10^{-8}$), using t-test: two-sample assuming equal variances.

Figure 7: NO induces collective invasion in MCF-7 breast cancer spheroids. BF images of 2-day MCF-7 breast cancer spheroids, embedded in collagen (A) at ($t = 0$) and (B) after 20 h exposure to 1 μM DETA/NO. Spheroid ROI segmentation is defined by red border, overlaid and numbered in red on BF images A and B. ROIs defined by blue border, overlaid on BF image B represent spheroid size and location at $t = 0$. Magnification 4X, scale bar = 500 μm . (C) A scatter plot of the correlation between elongation factor and migration distance of individual breast cancer

spheroids upon the exposure to 1 μ M DETA/NO (brown squares) as compared to control (blue diamonds) at $t = 20$ h, $n = 54$.

Figure 8: HeLa cell spontaneous invasion image analysis. BF images of 3-day HeLa spheroids, 16 h after embedding in collagen (A). Magnification 10X. Spheroid invasion area and disengaged cells are defined by red border, spheroid size at $t = 0$ is defined by blue border, mean invasion distance from spheroid center of mass is indicated by yellow arrows and disengaged cells are indicated by black arrows. Plot the increase over time of the mean invasion distance from spheroid center of mass (B) and total invasion area (C). The curves represent spheroid #1 (blue diamonds), spheroid #2 (brown squares), spheroid #3 (green triangles) and spheroid #4 (purple Xs). (D) Bar chart of the main (blue) and separated cell (brown) invasion area increase over time. (E) Distribution histogram of the cumulative number of separated cells per spheroid during 20 h of invasion process, $n = 126$.

DISCUSSION:

It is well documented that living organisms, characterized by their complex 3D multicellular organization are quite distinct from the commonly used 2D monolayer cultured cells, emphasizing the crucial need to use cellular models which better mimic the functions and processes of the living organism for drug screening. Recently, multicellular spheroids, organotypic cultures, organoids and organs-on-a-chip have been introduced⁸ for the use in standardized drug discovery. However, the 3D multicellular model's great complexity significantly jeopardizes its robustness, parallelization and data analysis which are crucial for assay efficiency.

Quantitative evaluation of invasion capacity typically measures the movement of cells through hydrogel materials. In order to measure the tumor invasion using traditional micro-well plates, large numbers of cancer cells are seeded in round bottom plates and forced to aggregate by centrifugation^{21,22}. These plates restrict cell/spheroid interaction in adjoining wells, while the round bottom obstructs the optical quality and complicates image acquisition. In other methods, individual cells randomly encapsulated within the hydrogel, grow and function in a 3D environment but do not necessarily develop into mature spheroids^{23,24}. Moreover, complicated procedures for cell positioning within hydrogel are required, like magnetic force-based cell patterning²⁵ or two-photon laser irradiation of bioactive hydrogels²⁶.

The HMCA-based technology presented herein proves to be advantageous over the above methods: cell positioning, spontaneous aggregation and creation of spheroids from few dispersed cells can be easily achieved, enabling the use of valuable limited cellular sample (*e.g.*, cancer stem-like cells or primary cells derived from patient specimens). The system has control over both the nature of the cells that compose the spheroids as well as over their exact spatial location during long term experiments. In addition, the flat bottom of the MC facilitates the generation of numerous spheroids on the same focal plan, hence rapid illumination and image acquisition of large areas via a wide field microscope is possible, eliminating the need for complicated time-consuming confocal microscopy. The system is easy to handle and its

practicality feasible. By applying simple operational procedures, we achieved high occupancy of spheroid populations in which approximately 50% of the spheroids have comparable size and a reliable analysis of cancer cell invasion capacity. In addition, the effect of drugs on invasion capacity can be analyzed simultaneously with their cytostatic and/or cytotoxic effects by using high-content analysis approach together with HMCA device cultured with numerous spheroids. Moreover, in the HMCA, all cellular elements share the same space and medium, making it possible to investigate spheroid-spheroid interaction which is usually mediated via cell-secreted cytokines, chemokines, hormones and the ECM²⁷. This cross-talk facilitates the survival and the function of individual cells/small cell clusters in macro-well volume.

A critical step in the execution of the protocol is the addition of ECM mixture on top of the spheroids and validating its proper polymerization. The spheroids will not show migratory behavior even if they are embedded within ECM, unless assembly and cross-linking occur, and appropriate collagen fibers are formed. The collagen fibers can be observed by BF illumination, and we advise checking the plate under a microscope to confirm the creation of collagen fibers at the end of this phase. Since the number of spheroids is dependent on initial cell concentration and the percent of occupied MCs, the array should be checked after initial cell loading, and if cell occupancy is not optimal, re-seeding of the same array may be performed. Indeed, the size and geometry of the HMCA described herein were designed to accommodate relatively small cell clusters (up to 150 μm in diameter). This could be considered a limitation since designing a new type of array will be necessary for analyzing cell migration from larger cell structures.

The current platform utilizes minimal cell number and small reagent volume, while at the same time providing a large sample size (thousands of spheroids per plate). In order to analyze 12 different compounds for anti-metastatic activity, 2 single 6-well HMCA based plates would be required, yielding the results from about 5000 spheroids, while at least fifty 96-well plates would be needed to achieve the same outcomes. The ability to analyze the migration at individual-object resolution in the HMCA provides a high level of statistical robustness and accuracy, enabling the study of structural and functional invasion heterogeneity in numerous spheroids.

This study uniquely demonstrates the collective invasion of breast cancer spheroid populations upon the exposure to DETA/NO. The cell clusters of MCF7 cells show amoeboid migratory phenotype, and quantitative changes in the morphology and location of each spheroid can be automatically attained. To the best of our knowledge, this is the first arrayed system that facilitates monitoring and analysis of collective invasion in numerous 3D structures. By analyzing the relative directions and the invasion distance for each spheroid, it is possible to study the mutual interaction between spheroids within the population. Additionally, the established influence of extracellular microenvironment factors on cancer cell behavior²⁸ is illustrated here. Among these factors, the stiffness and composition of the microenvironment has been shown to strongly influence cell migration. HMCA technology provides a defined, biomimetic, *in vitro* platform, in which these properties of the ECM can be easily accessed and

controlled. The stiffness of pure collagen type I hydrogel at the concentration of 3 mg/mL which was used in this study, is reported to be approximately 50-600 Pa²⁹⁻³¹ and the addition of HA (20 µg/mL; 0.4 wt %) did not change the stiffness of the hydrogel significantly^{32,33}. Thus, the suppressive effect of medium molecular weight (MMW)-HA on the invasion of 3D HeLa spheroids which was demonstrated here is not due to stiffness changes. These results are in agreement with previous studies which showed a bimodal effect of HA on cancer cell invasion with high dependency on HA molecular weight³⁴⁻³⁷.

Future applications of the methods include side by side multi cell type culturing of tumor and stromal cells in different regions within the macro-well, and retrieval of specific spheroids for downstream molecular analysis.

ACKNOWLEDGMENTS:

This work is supported by the bequest of Moshe Shimon and Judith Weisbrodt.

DISCLOSURES:

The authors declare that they have no competing financial interests.

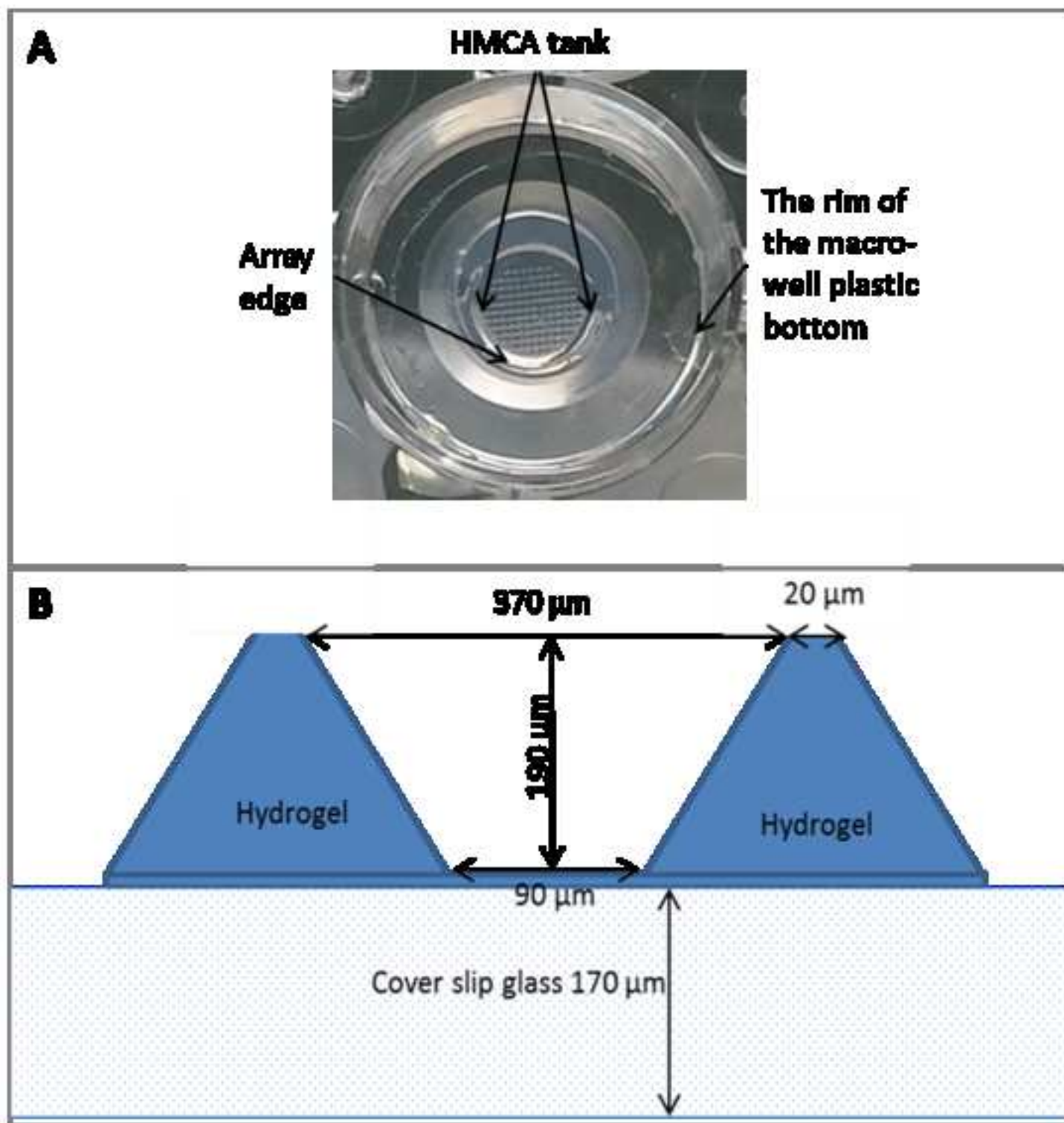
REFERENCES:

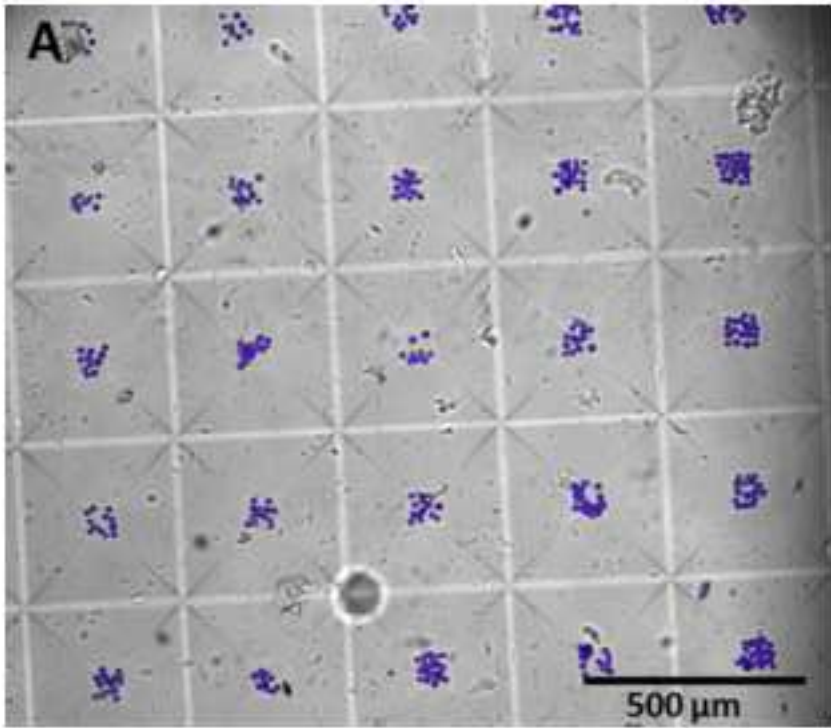
1. Guan, X. Cancer metastases: challenges and opportunities. *Acta pharmaceutica Sinica. B.* **5** (5), 402–18, doi: 10.1016/j.apsb.2015.07.005 (2015).
2. Sapudom, J. *et al.* The phenotype of cancer cell invasion controlled by fibril diameter and pore size of 3D collagen networks. *Biomaterials.* **52**, 367–375, doi: 10.1016/j.biomaterials.2015.02.022 (2015).
3. Portillo-Lara, R., Annabi, N. Microengineered cancer-on-a-chip platforms to study the metastatic microenvironment. *Lab on a chip.* **16** (21), 4063–4081, doi: 10.1039/c6lc00718j (2016).
4. Gkoutela, S., Aceto, N. Stem-like features of cancer cells on their way to metastasis. *Biology Direct.* **11** (1), 33, doi: 10.1186/s13062-016-0135-4 (2016).
5. Kramer, N. *et al.* In vitro cell migration and invasion assays. *Mutation Research/Reviews in Mutation Research.* **752** (1), 10–24, doi: 10.1016/j.mrrev.2012.08.001 (2013).
6. Guzman, A., Sánchez Alemany, V., Nguyen, Y., Zhang, C.R., Kaufman, L.J. A novel 3D in vitro metastasis model elucidates differential invasive strategies during and after breaching basement membrane. *Biomaterials.* **115**, 19–29, doi: 10.1016/j.biomaterials.2016.11.014 (2017).
7. Lee, E., Song, H.-H.G., Chen, C.S. Biomimetic on-a-chip platforms for studying cancer metastasis. *Current opinion in chemical engineering.* **11**, 20–27, doi: 10.1016/j.coche.2015.12.001 (2016).
8. Mittler, F., Obeid, P., Rulina, A. V., Haguët, V., Gidrol, X., Balakirev, M.Y. High-Content Monitoring of Drug Effects in a 3D Spheroid Model. *Frontiers in Oncology.* **7**, 293, doi: 10.3389/fonc.2017.00293 (2017).
9. Evensen, N.A. *et al.* Development of a High-Throughput Three-Dimensional Invasion Assay for Anti-Cancer Drug Discovery. *PLoS ONE.* **8** (12), e82811, doi:

10.1371/journal.pone.0082811 (2013).

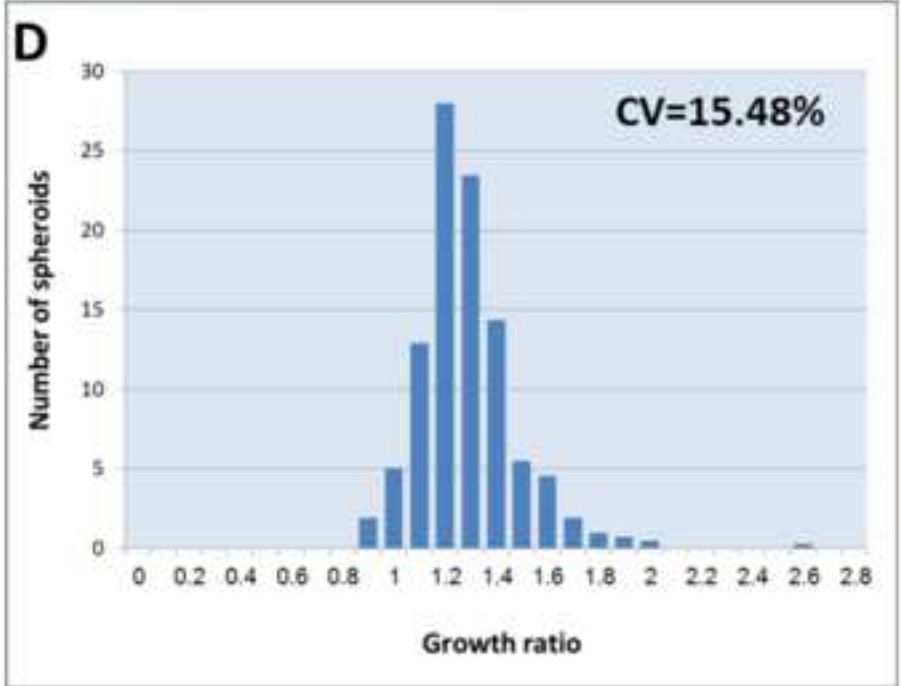
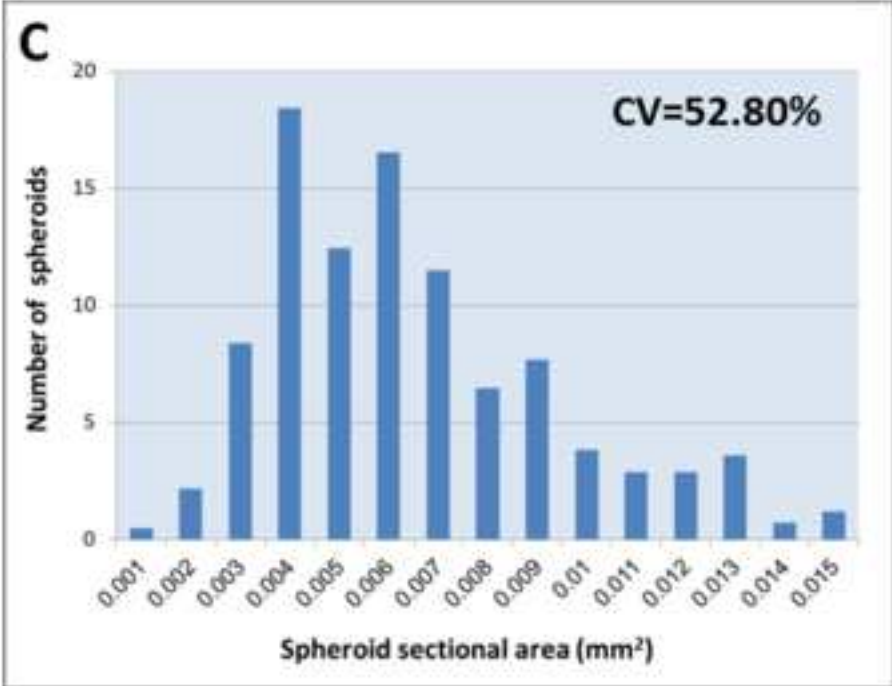
10. Aw Yong, K.M., Li, Z., Merajver, S.D., Fu, J. Tracking the tumor invasion front using long-term fluidic tumoroid culture. *Scientific Reports*. **7** (1), 10784, doi: 10.1038/s41598-017-10874-1 (2017).
11. Mi, S. *et al.* Microfluidic co-culture system for cancer migratory analysis and anti-metastatic drugs screening. *Scientific Reports*. **6** (1), 35544, doi: 10.1038/srep35544 (2016).
12. Chung, S., Sudo, R., Mack, P.J., Wan, C.-R., Vickerman, V., Kamm, R.D. Cell migration into scaffolds under co-culture conditions in a microfluidic platform. *Lab on a chip*. **9** (2), 269–75, doi: 10.1039/b807585a (2009).
13. Krakhmal, N. V, Zavyalova, M. V, Denisov, E. V, Vtorushin, S. V, Perelmuter, V.M. Cancer Invasion: Patterns and Mechanisms. *Acta naturae*. **7** (2), 17–2814. Lintz, M., Muñoz, A., Reinhart-King, C.A. The Mechanics of Single Cell and Collective Migration of Tumor Cells. *Journal of Biomechanical Engineering*. **139** (2), 21005, doi: 10.1115/1.4035121 (2017).
15. Afrimzon, E. *et al.* Hydrogel microstructure live-cell array for multiplexed analyses of cancer stem cells, tumor heterogeneity and differential drug response at single-element resolution. *Lab on a Chip*. **16** (6), 1047–1062, doi: 10.1039/C6LC00014B (2016).
16. Shafran, Y. *et al.* Nitric oxide is cytoprotective to breast cancer spheroids vulnerable to estrogen-induced apoptosis. *Oncotarget*. **8** (65), 108890–108911, doi: 10.18632/oncotarget.21610 (2017).
17. Sato, H., Idiris, A., Miwa, T., Kumagai, H. Microfabric Vessels for Embryoid Body Formation and Rapid Differentiation of Pluripotent Stem Cells. *Scientific Reports*. **6** (1), 31063, doi: 10.1038/srep31063 (2016).
18. Lee, K. *et al.* Gravity-oriented microfluidic device for uniform and massive cell spheroid formation. *Biomicrofluidics*. **6** (1), 14114, doi: 10.1063/1.3687409 (2012).
19. Zaretsky, I. *et al.* Monitoring the dynamics of primary T cell activation and differentiation using long term live cell imaging in microwell arrays. *Lab on a Chip*. **12** (23), 5007, doi: 10.1039/c2lc40808b (2012).
20. Khan, N., Syed, D.N., Ahmad, N., Mukhtar, H. Fisetin: a dietary antioxidant for health promotion. *Antioxidants & redox signaling*. **19** (2), 151–62, doi: 10.1089/ars.2012.4901 (2013).
21. Lee, G.H. *et al.* Networked concave microwell arrays for constructing 3D cell spheroids. *Biofabrication*. **10** (1), 15001, doi: 10.1088/1758-5090/aa9876 (2017).
22. Vinci, M., Box, C., Eccles, S.A. Three-dimensional (3D) tumor spheroid invasion assay. *Journal of visualized experiments : JoVE*. (99), e52686, doi: 10.3791/52686 (2015).
23. Toh, Y.-C., Raja, A., Yu, H., van Noort, D. A 3D Microfluidic Model to Recapitulate Cancer Cell Migration and Invasion. *Bioengineering*. **5** (2), 29, doi: 10.3390/bioengineering5020029 (2018).
24. Sugimoto, M., Kitagawa, Y., Yamada, M., Yajima, Y., Utoh, R., Seki, M. Micropassage-embedding composite hydrogel fibers enable quantitative evaluation of cancer cell invasion under 3D coculture conditions. *Lab on a Chip*. **18** (9), 1378–1387, doi: 10.1039/C7LC01280B (2018).
25. Yamamoto, S., Hotta, M.M., Okochi, M., Honda, H. Effect of Vascular Formed Endothelial

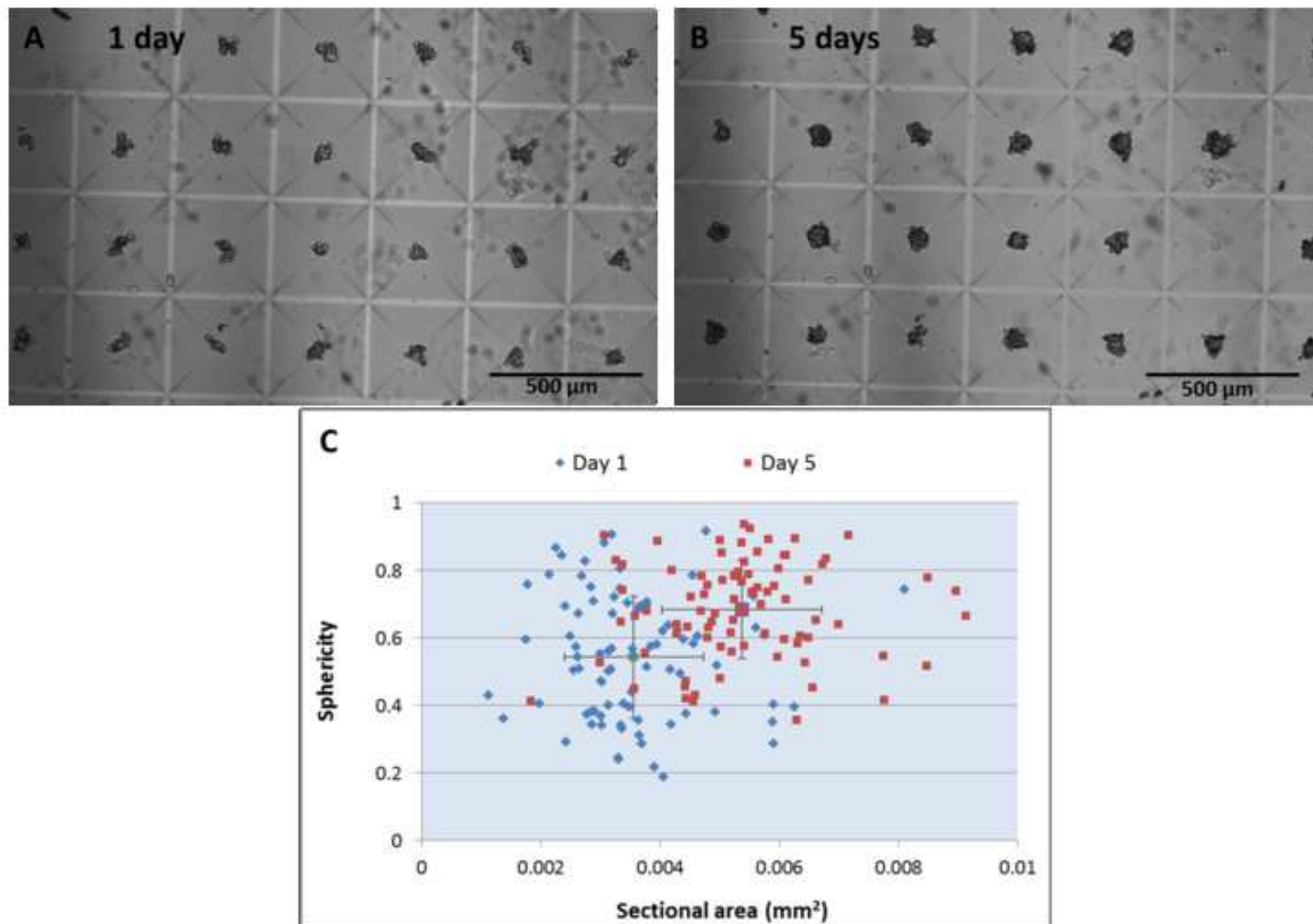
- Cell Network on the Invasive Capacity of Melanoma Using the In Vitro 3D Co-Culture Patterning Model. *PLoS ONE*. **9** (7), e103502, doi: 10.1371/journal.pone.0103502 (2014).
26. Lee, S.-H., Moon, J.J., West, J.L. Three-dimensional micropatterning of bioactive hydrogels via two-photon laser scanning photolithography for guided 3D cell migration. *Biomaterials*. **29** (20), 2962–2968, doi: 10.1016/j.biomaterials.2008.04.004 (2008).
27. Gschwind, A., Zwick, E., Prenzel, N., Leserer, M., Ullrich, A. Cell communication networks: epidermal growth factor receptor transactivation as the paradigm for interreceptor signal transmission. *Oncogene*. **20** (13), 1594–1600, doi: 10.1038/sj.onc.1204192 (2001).
28. Jiang, K., Dong, C., Xu, Y., Wang, L. Microfluidic-based biomimetic models for life science research. *RSC Advances*. **6** (32), 26863–26873, doi: 10.1039/C6RA05691A (2016).
29. Mason, B.N., Starchenko, A., Williams, R.M., Bonassar, L.J., Reinhart-King, C.A. Tuning three-dimensional collagen matrix stiffness independently of collagen concentration modulates endothelial cell behavior. *Acta biomaterialia*. **9** (1), 4635–44, doi: 10.1016/j.actbio.2012.08.007 (2013).
30. Raub, C.B., Putnam, A.J., Tromberg, B.J., George, S.C. Predicting bulk mechanical properties of cellularized collagen gels using multiphoton microscopy. *Acta Biomaterialia*. **6** (12), 4657–4665, doi: 10.1016/j.actbio.2010.07.004 (2010).
31. Paszek, M.J. *et al.* Tensional homeostasis and the malignant phenotype. *Cancer Cell*. **8** (3), 241–254, doi: 10.1016/j.ccr.2005.08.010 (2005).
32. Rao, S.S., DeJesus, J., Short, A.R., Otero, J.J., Sarkar, A., Winter, J.O. Glioblastoma Behaviors in Three-Dimensional Collagen-Hyaluronan Composite Hydrogels. *ACS Applied Materials & Interfaces*. **5** (19), 9276–9284, doi: 10.1021/am402097j (2013).
33. Kreger, S.T., Voytik-Harbin, S.L. Hyaluronan concentration within a 3D collagen matrix modulates matrix viscoelasticity, but not fibroblast response. *Matrix Biology*. **28** (6), 336–346, doi: 10.1016/j.matbio.2009.05.001 (2009).
34. Chanmee, T., Ontong, P., Itano, N. Hyaluronan: A modulator of the tumor microenvironment. *Cancer Letters*. **375** (1), 20–30, doi: 10.1016/J.CANLET.2016.02.031 (2016).
35. Zhao, Y. *et al.* Modulating Three-Dimensional Microenvironment with Hyaluronan of Different Molecular Weights Alters Breast Cancer Cell Invasion Behavior. *ACS Applied Materials & Interfaces*. **9** (11), 9327–9338, doi: 10.1021/acsami.6b15187 (2017).
36. Wu, M. *et al.* A novel role of low molecular weight hyaluronan in breast cancer metastasis. *The FASEB Journal*. **29** (4), 1290–1298, doi: 10.1096/fj.14-259978 (2015).
37. Fisher, G.J. Cancer resistance, high molecular weight hyaluronic acid, and longevity. *Journal of cell communication and signaling*. **9** (1), 91–2, doi: 10.1007/s12079-015-0278-6 (2015).

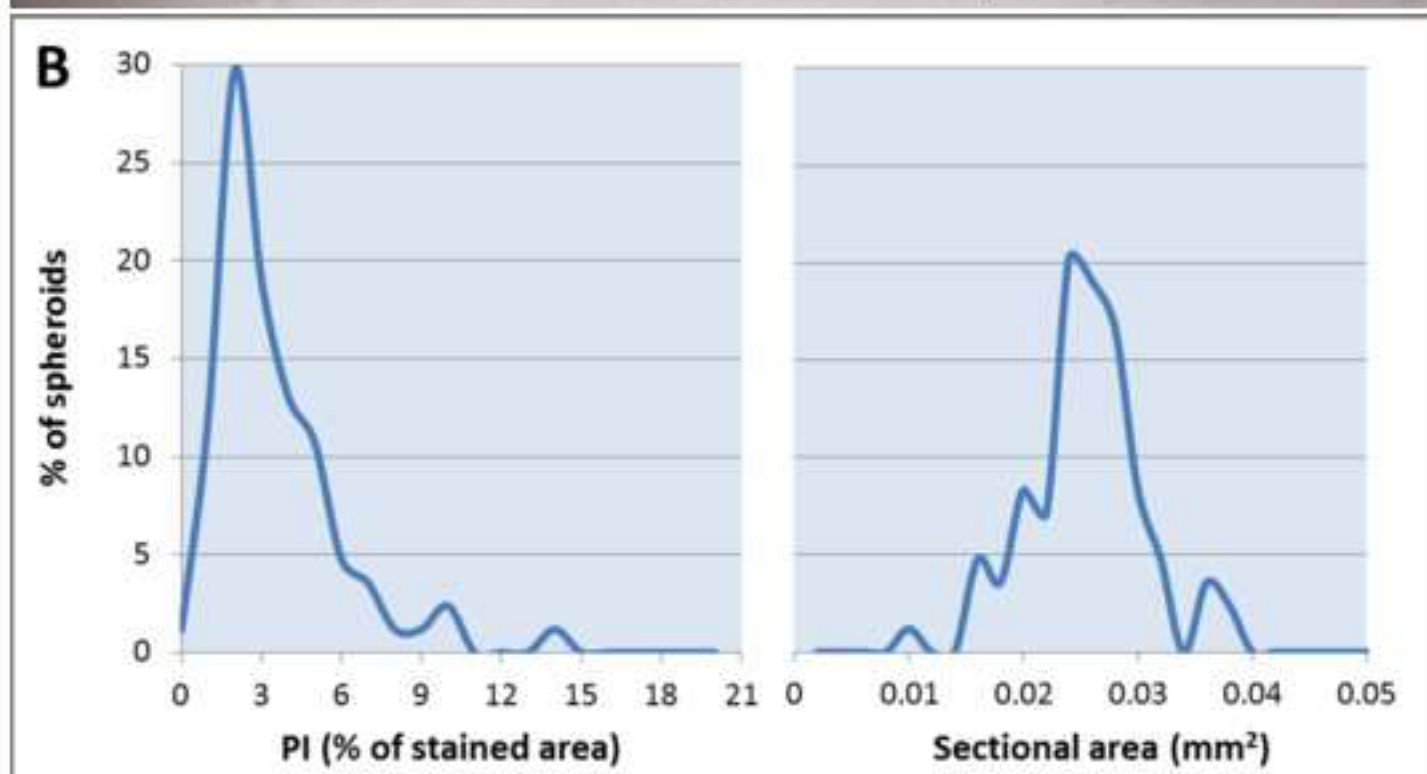
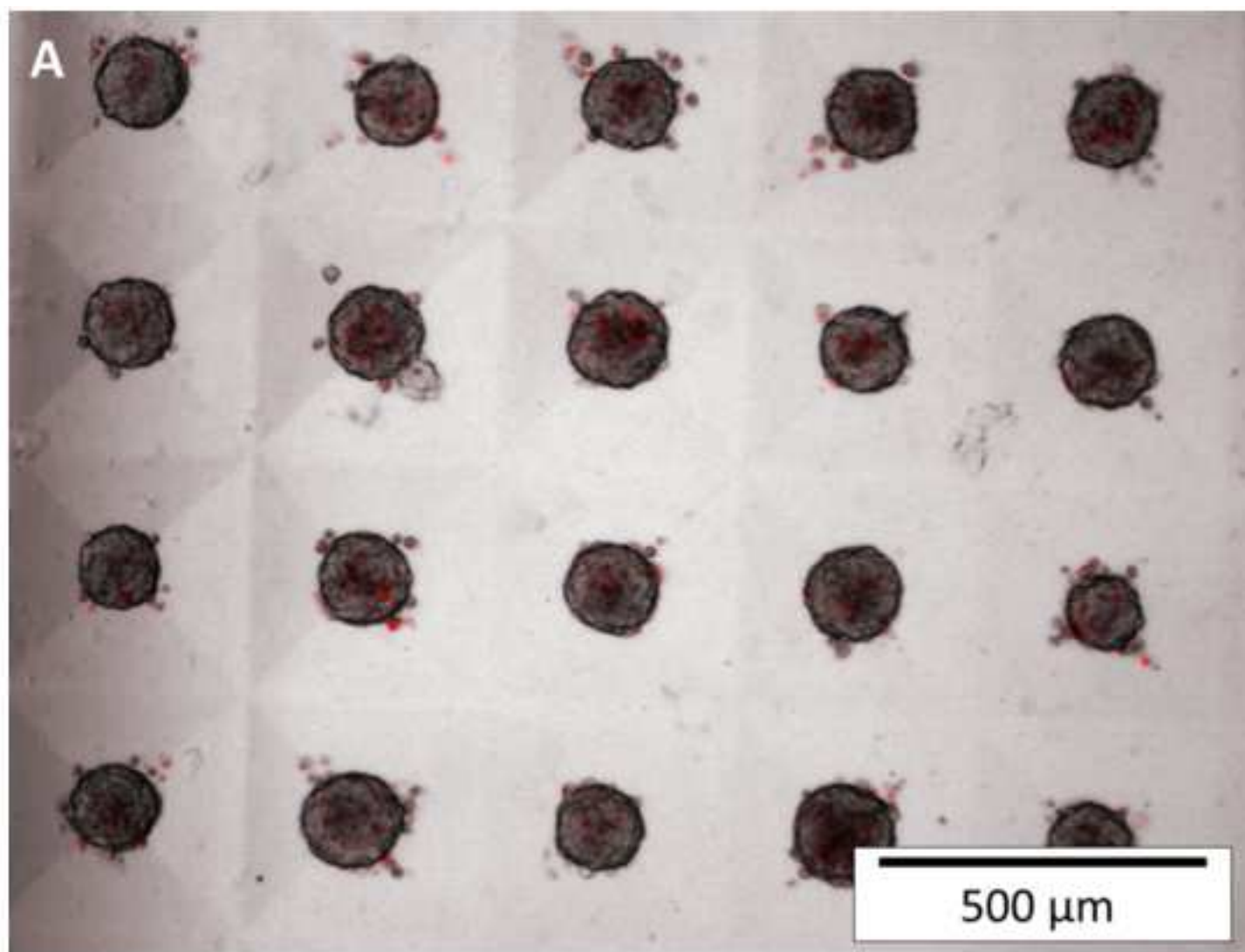


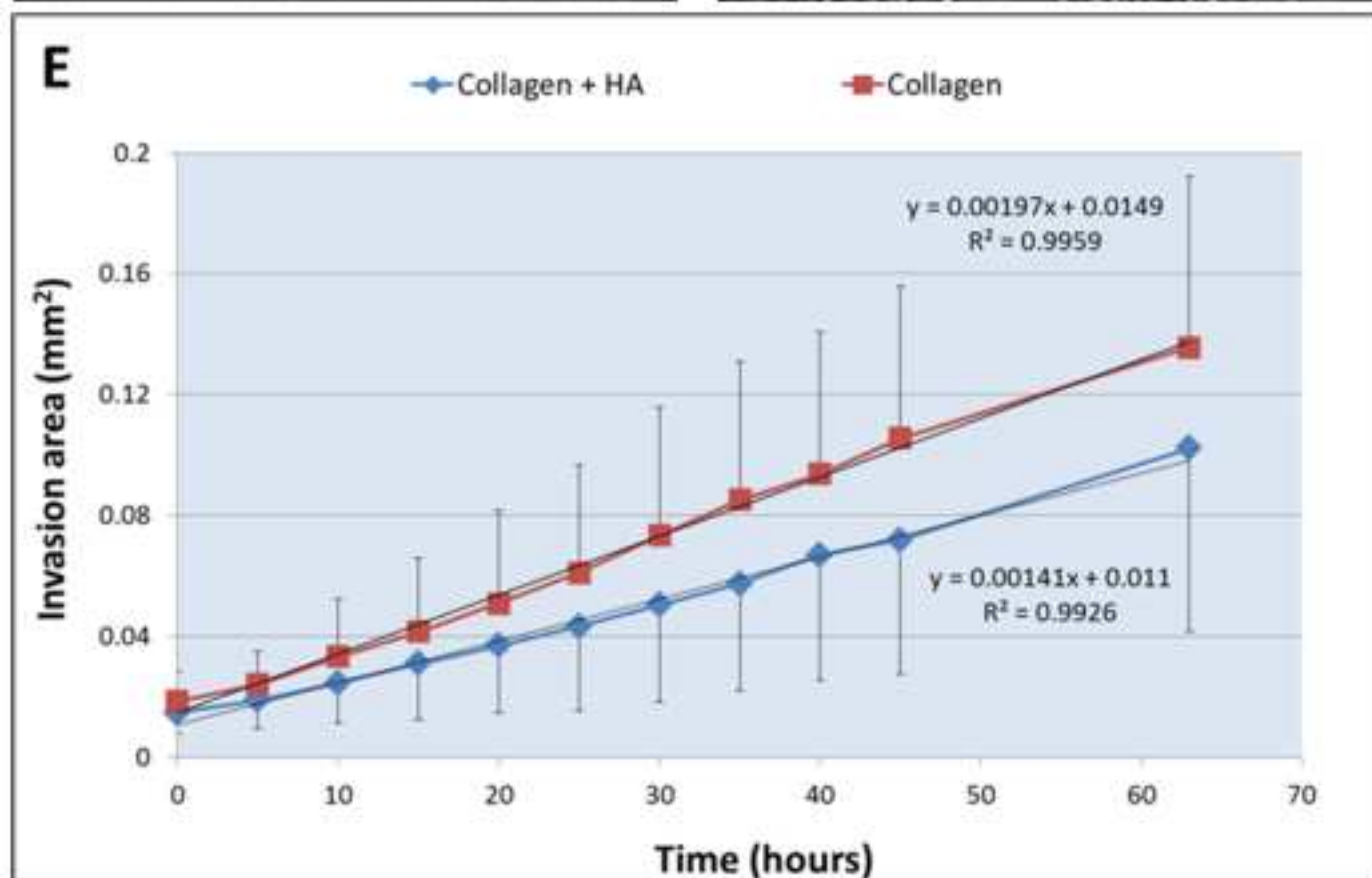
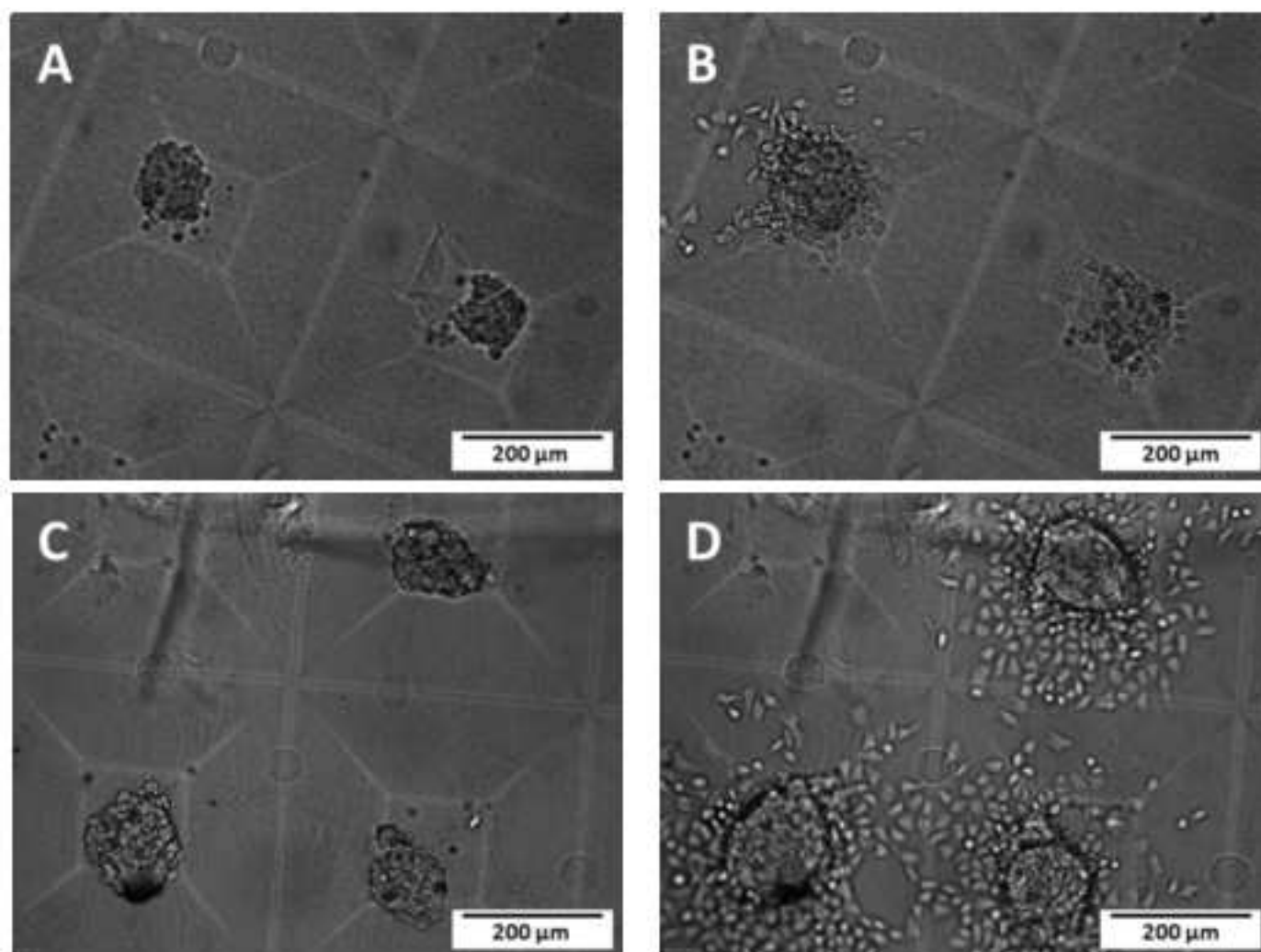


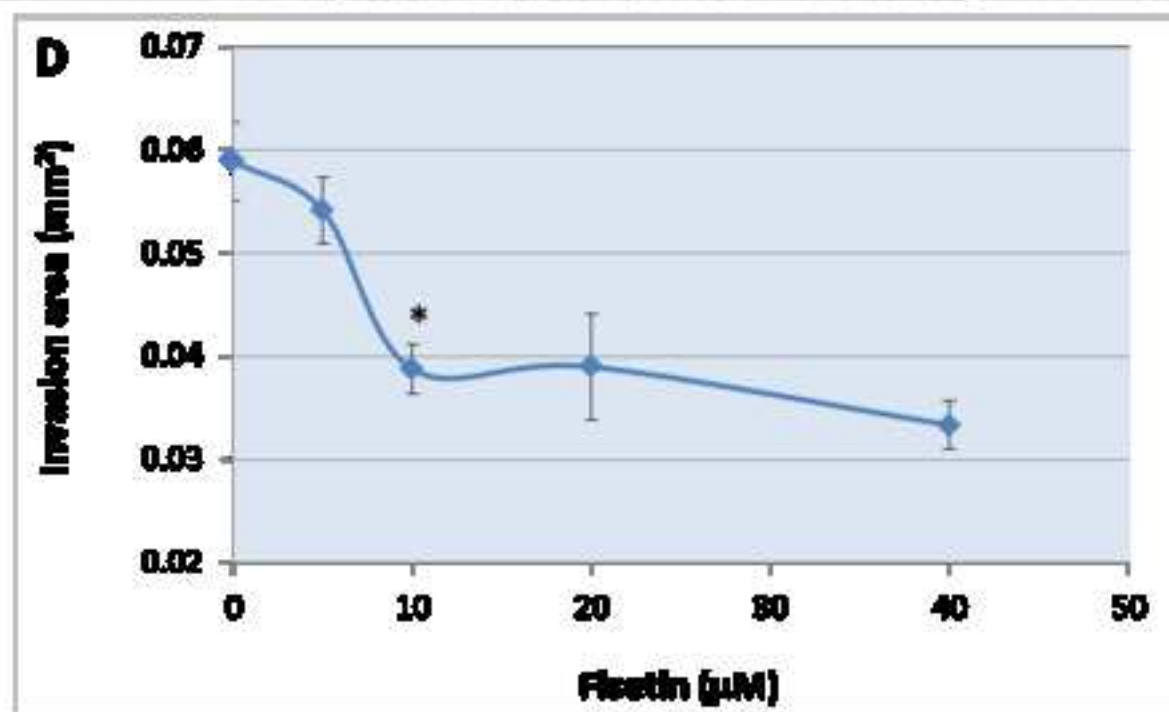
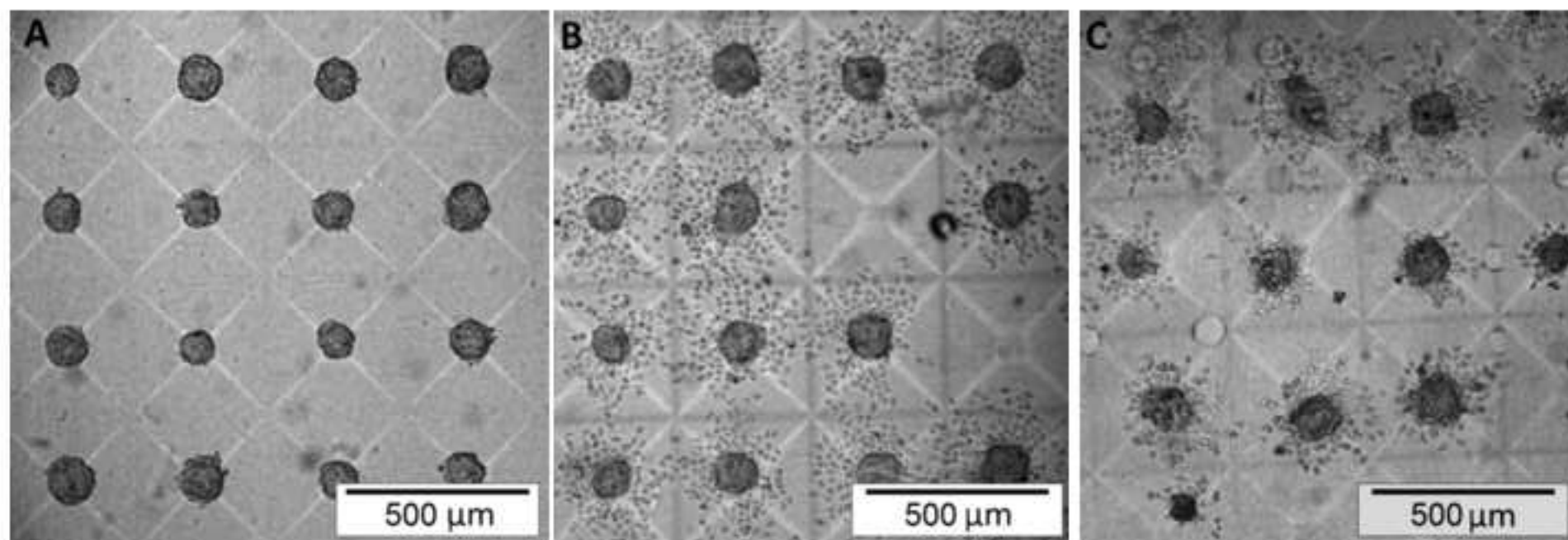
Well #	Average number of cells/MC	Coefficient of variation (CV) within macro-wells (%)
1	12.70 \pm 7.85	61.80
2	18.31 \pm 6.06	33.12
3	18.62 \pm 6.62	35.59
4	13.16 \pm 5.11	38.83
5	9.48 \pm 3.67	38.71
6	16.43 \pm 8.53	51.93
Average	14.78 \pm 3.60	43.33 \pm 11.14
Coefficient of variation (CV) between macro-wells		24.37%

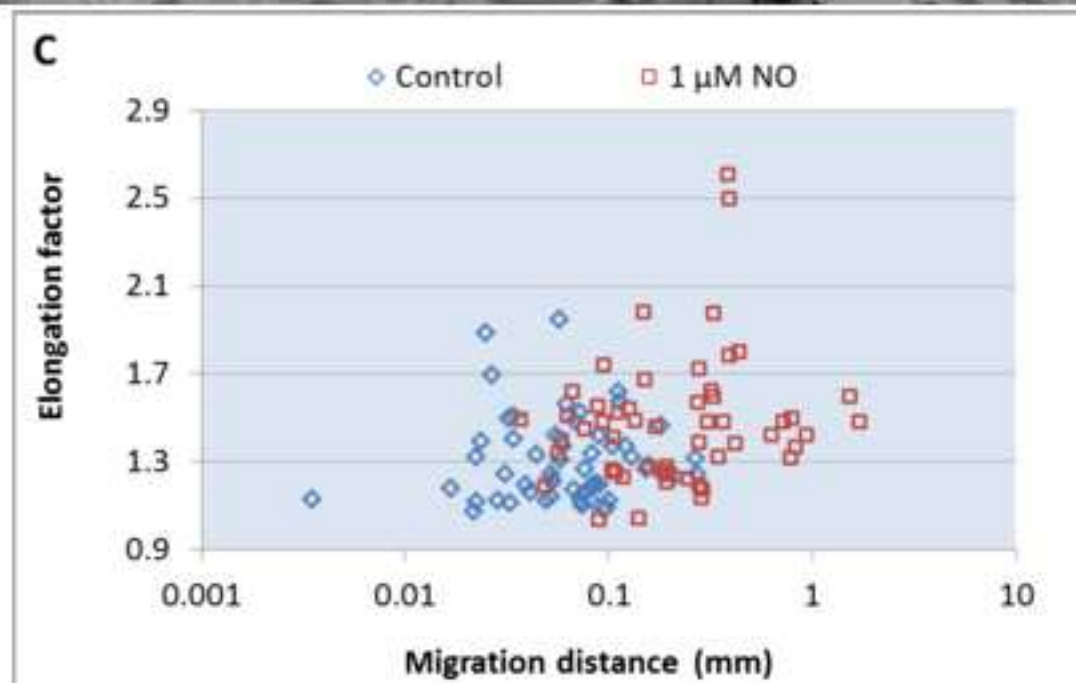
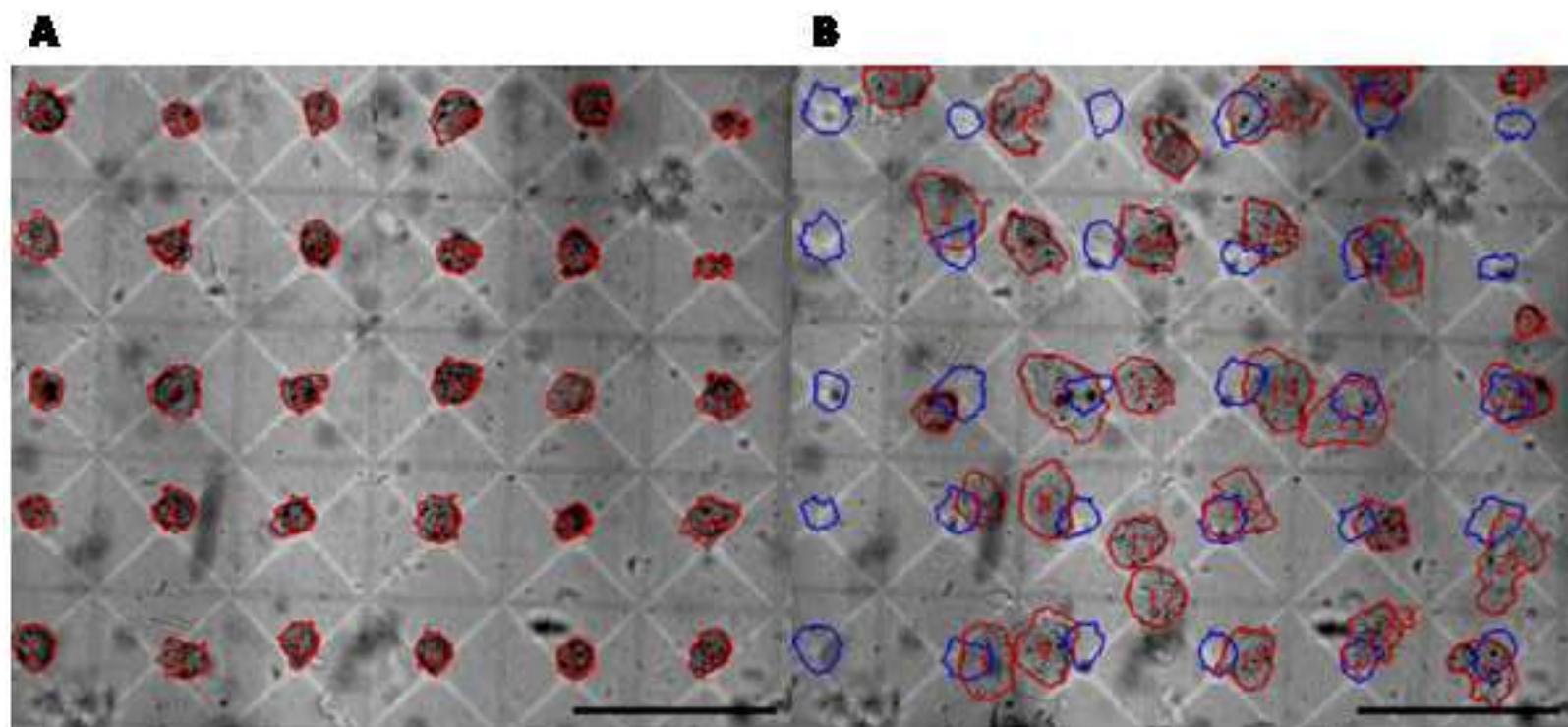


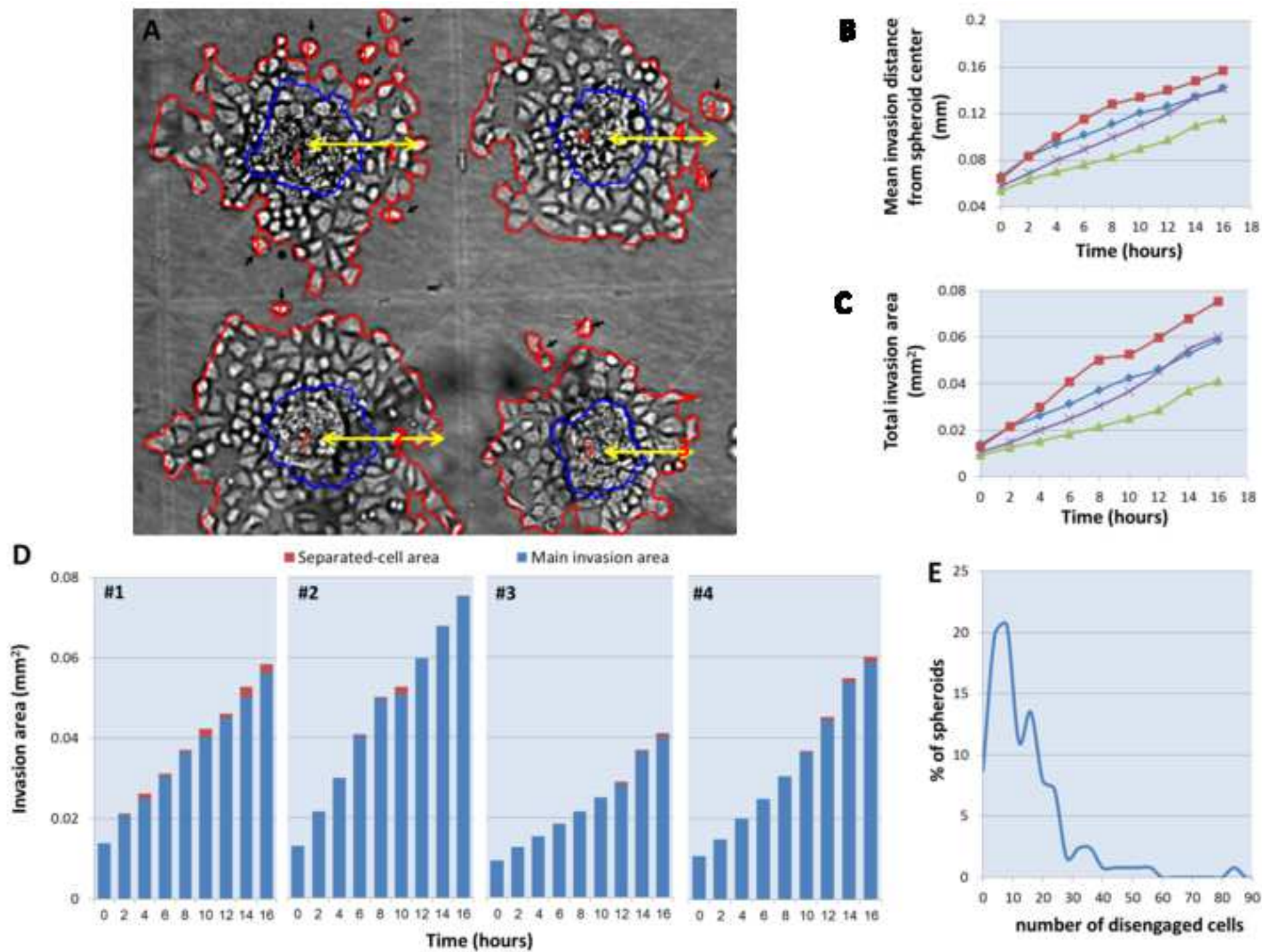












Name of Material/ Equipment	Company	Catalog Number
6 Micro-well Glass Bottom Plates with 14 mm micro-well #1.5 cover glass	Cellvis	P06-14-1.5-N
UltraPure Low Melting Point Agarose	Invitrogen	16520100
Trypsin EDTA solution B	Biological Industries	03-052-1A
DMEM medium, high glucose	Biological Industries	01-055-1A
Special Newborn Calf Serum (NBCS)	Biological Industries	04-122-1A
DPBS (10X), no calcium, no magnesium	Biological Industries	02-023-5A
NaOH, anhydrous	Sigma-Aldrich	S5881-500G
Cultrex Type I collagen from rat tail, 5mg/ml	Trevigen	3440-100-01
Hyaluronic acid sodium salt	Sigma-Aldrich	H5542-10MG
Fisetin	Sigma-Aldrich	F505-100MG
DETA/NO	Enzo Life Sciences	alx-430-014-m005
PI	Sigma-Aldrich	P4170
Dymax 5000-EC UV flood lamp complete system with light shield & Dymax 400 Watt EC power supply	Dymax Corporation	PN 39823
Inverted IX81 microscope	Olympus	
Incubator for microscope	Life Imaging Services	

Sub-micron motorized stage type SCAN-IM	Marzhauser Wetzlar GmbH
14-bit, ORCA II C4742-98 cooled camera	Hamamatsu Photonics
Fluorescent filter cube for PI detection	Chroma Technology Corporation
The Olympus Cell [^] P operating software	Olympus
Matlab R2014B analysis software	Mathworks
Excel software	Microsoft

Comments/Description

Commercial glass bottom plates
which are used for HMCA
embossing

A solution of 6% agarose is warmed
up to 80°C before use, a solution of
1% agarose is warmed to 37°C

Warmed to 37°C before use

Warmed to 37°C before use

Heat Inactivated

Kept on ice before use

Used for the preparation of 1M

NaOH solution

Kept on ice before use

Kept on ice before use

Added to the culture medium,
invasion inhibitor

Added to the culture medium, nitric
oxide donor

Used at very low concentration
without the need for washing

Used for HMCA plate sterilization by
UV

Used for automatic image
acquisition

Essential for time lapse experiments
with image acquisition, pre adjusted
to 37°C, 5% CO₂ and keeping a
humidified atmosphere

Used to predetermine image acquisition areas, for automatic image acquisition

Highly sensitive, used for imaging

Filter cube specifications: excitation filter 530-550 nm, dichroic mirror 565 nm long pass and emission filter 600-660 nm

Software used to control microscope, motorized stage, camera and image acquisition

Used to develop in house graphic user interface for image analysis

Used for data management, calculation, plot creation and statistics



1 Alewife Center #200
 Cambridge, MA 02140
 tel. 617.945.9051
 www.jove.com

ARTICLE AND VIDEO LICENSE AGREEMENT

Title of Article:

Analysis of cancer cell invasion and anti-metastatic drug screening
 using hydrogel microarray chamber array based plates.

Author(s):

Ravid-Hermesh Orit, Zurgil Domoni, Shofran Yana, Afrimzon Elena, Sobler Maria,

Item 1 (check one box): The Author elects to have the Materials be made available (as described at

http://www.jove.com/author) via: ☒ Standard Access ☐ Open Access

Item 2 (check one box):

- ☒ The Author is NOT a United States government employee.
- ☐ The Author is a United States government employee and the Materials were prepared in the course of his or her duties as a United States government employee.
- ☐ The Author is a United States government employee but the Materials were NOT prepared in the course of his or her duties as a United States government employee.

Hakuk Yaron,
 Eizig Zehavit,
 Deutsch Mordecha

ARTICLE AND VIDEO LICENSE AGREEMENT

1. **Defined Terms.** As used in this Article and Video License Agreement, the following terms shall have the following meanings: "Agreement" means this Article and Video License Agreement; "Article" means the article specified on the last page of this Agreement, including any associated materials such as texts, figures, tables, artwork, abstracts, or summaries contained therein; "Author" means the author who is a signatory to this Agreement; "Collective Work" means a work, such as a periodical issue, anthology or encyclopedia, in which the Materials in their entirety in unmodified form, along with a number of other contributions, constituting separate and independent works in themselves, are assembled into a collective whole; "CRC License" means the Creative Commons Attribution-Non Commercial-No Derivs 3.0 Unported Agreement, the terms and conditions of which can be found at: <http://creativecommons.org/licenses/by-nc-nd/3.0/legalcode>; "Derivative Work" means a work based upon the Materials or upon the Materials and other pre-existing works, such as a translation, musical arrangement, dramatization, fictionalization, motion picture version, sound recording, art reproduction, abridgment, condensation, or any other form in which the Materials may be recast, transformed, or adapted; "Institution" means the institution, listed on the last page of this Agreement, by which the Author was employed at the time of the creation of the Materials; "JoVE" means MyJoVE Corporation, a Massachusetts corporation and the publisher of *The Journal of Visualized Experiments*; "Materials" means the Article and / or the Video; "Parties" means the Author and JoVE; "Video" means any video(s) made by the Author, alone or in conjunction with any other parties, or by JoVE or its affiliates or agents, individually or in collaboration with the Author or any other parties, incorporating all or any portion of the Article, and in which the Author may or may not appear.

2. **Background.** The Author, who is the author of the Article, in order to ensure the dissemination and protection of the Article, desires to have the JoVE publish the Article and create and transmit videos based on the Article. In furtherance of such goals, the Parties desire to memorialize in this Agreement the respective rights of each Party in and to the Article and the Video.

3. **Grant of Rights in Article.** In consideration of JoVE agreeing to publish the Article, the Author hereby grants to JoVE, subject to Sections 4 and 7 below, the exclusive, royalty-free, perpetual (for the full term of copyright in the Article, including any extensions thereto) license (a) to publish, reproduce, distribute, display and store the Article in all forms, formats and media whether now known or hereafter developed (including without limitation in print, digital and electronic form) throughout the world, (b) to translate the Article into other languages, create adaptations, summaries or extracts of the Article or other Derivative Works (including, without limitation, the Video) or Collective Works based on all or any portion of the Article and exercise all of the rights set forth in (a) above in such translations, adaptations, summaries, extracts, Derivative Works or Collective Works and (c) to license others to do any or all of the above. The foregoing rights may be exercised in all media and formats, whether now known or hereafter devised, and include the right to make such modifications as are technically necessary to exercise the rights in other media and formats. If the "Open Access" box has been checked in Item 1 above, JoVE and the Author hereby grant to the public all such rights in the Article as provided in, but subject to all limitations and requirements set forth in, the CRC License.

ARTICLE AND VIDEO LICENSE AGREEMENT

4. **Retention of Rights in Article.** Notwithstanding the exclusive license granted to JoVE in **Section 3** above, the Author shall, with respect to the Article, retain the non-exclusive right to use all or part of the Article for the non-commercial purpose of giving lectures, presentations or teaching classes, and to post a copy of the Article on the Institution's website or the Author's personal website, in each case provided that a link to the Article on the JoVE website is provided and notice of JoVE's copyright in the Article is included. All non-copyright intellectual property rights in and to the Article, such as patent rights, shall remain with the Author.

5. **Grant of Rights in Video – Standard Access.** This **Section 5** applies if the "Standard Access" box has been checked in **Item 1** above or if no box has been checked in **Item 1** above. In consideration of JoVE agreeing to produce, display or otherwise assist with the Video, the Author hereby acknowledges and agrees that, Subject to **Section 7** below, JoVE is and shall be the sole and exclusive owner of all rights of any nature, including, without limitation, all copyrights, in and to the Video. To the extent that, by law, the Author is deemed, now or at any time in the future, to have any rights of any nature in or to the Video, the Author hereby disclaims all such rights and transfers all such rights to JoVE.

6. **Grant of Rights in Video – Open Access.** This **Section 6** applies only if the "Open Access" box has been checked in **Item 1** above. In consideration of JoVE agreeing to produce, display or otherwise assist with the Video, the Author hereby grants to JoVE, subject to **Section 7** below, the exclusive, royalty-free, perpetual (for the full term of copyright in the Article, including any extensions thereto) license (a) to publish, reproduce, distribute, display and store the Video in all forms, formats and media whether now known or hereafter developed (including without limitation in print, digital and electronic form) throughout the world, (b) to translate the Video into other languages, create adaptations, summaries or extracts of the Video or other Derivative Works or Collective Works based on all or any portion of the Video and exercise all of the rights set forth in (a) above in such translations, adaptations, summaries, extracts, Derivative Works or Collective Works and (c) to license others to do any or all of the above. The foregoing rights may be exercised in all media and formats, whether now known or hereafter devised, and include the right to make such modifications as are technically necessary to exercise the rights in other media and formats. For any Video to which this **Section 6** is applicable, JoVE and the Author hereby grant to the public all such rights in the Video as provided in, but subject to all limitations and requirements set forth in, the CRC License.

7. **Government Employees.** If the Author is a United States government employee and the Article was prepared in the course of his or her duties as a United States government employee, as indicated in **Item 2** above, and any of the licenses or grants granted by the Author hereunder exceed the scope of the 17 U.S.C. 403, then the rights granted hereunder shall be limited to the maximum rights permitted under such

statute. In such case, all provisions contained herein that are not in conflict with such statute shall remain in full force and effect, and all provisions contained herein that do so conflict shall be deemed to be amended so as to provide to JoVE the maximum rights permissible within such statute.

8. **Likeness, Privacy, Personality.** The Author hereby grants JoVE the right to use the Author's name, voice, likeness, picture, photograph, image, biography and performance in any way, commercial or otherwise, in connection with the Materials and the sale, promotion and distribution thereof. The Author hereby waives any and all rights he or she may have, relating to his or her appearance in the Video or otherwise relating to the Materials, under all applicable privacy, likeness, personality or similar laws.

9. **Author Warranties.** The Author represents and warrants that the Article is original, that it has not been published, that the copyright interest is owned by the Author (or, if more than one author is listed at the beginning of this Agreement, by such authors collectively) and has not been assigned, licensed, or otherwise transferred to any other party. The Author represents and warrants that the author(s) listed at the top of this Agreement are the only authors of the Materials. If more than one author is listed at the top of this Agreement and if any such author has not entered into a separate Article and Video License Agreement with JoVE relating to the Materials, the Author represents and warrants that the Author has been authorized by each of the other such authors to execute this Agreement on his or her behalf and to bind him or her with respect to the terms of this Agreement as if each of them had been a party hereto as an Author. The Author warrants that the use, reproduction, distribution, public or private performance or display, and/or modification of all or any portion of the Materials does not and will not violate, infringe and/or misappropriate the patent, trademark, intellectual property or other rights of any third party. The Author represents and warrants that it has and will continue to comply with all government, institutional and other regulations, including, without limitation all institutional, laboratory, hospital, ethical, human and animal treatment, privacy, and all other rules, regulations, laws, procedures or guidelines, applicable to the Materials, and that all research involving human and animal subjects has been approved by the Author's relevant institutional review board.

10. **JoVE Discretion.** If the Author requests the assistance of JoVE in producing the Video in the Author's facility, the Author shall ensure that the presence of JoVE employees, agents or independent contractors is in accordance with the relevant regulations of the Author's institution. If more than one author is listed at the beginning of this Agreement, JoVE may, in its sole discretion, elect not take any action with respect to the Article until such time as it has received complete, executed Article and Video License Agreements from each such author. JoVE reserves the right, in its absolute and sole discretion and without giving any reason therefore, to accept or decline any work submitted to JoVE. JoVE and its employees, agents and independent contractors shall have

ARTICLE AND VIDEO LICENSE AGREEMENT

full, unfettered access to the facilities of the Author or of the Author's institution as necessary to make the Video, whether actually published or not. JoVE has sole discretion as to the method of making and publishing the Materials, including, without limitation, to all decisions regarding editing, lighting, filming, timing of publication, if any, length, quality, content and the like.

11. Indemnification. The Author agrees to indemnify JoVE and/or its successors and assigns from and against any and all claims, costs, and expenses, including attorney's fees, arising out of any breach of any warranty or other representations contained herein. The Author further agrees to indemnify and hold harmless JoVE from and against any and all claims, costs, and expenses, including attorney's fees, resulting from the breach by the Author of any representation or warranty contained herein or from allegations or instances of violation of intellectual property rights, damage to the Author's or the Author's institution's facilities, fraud, libel, defamation, research, equipment, experiments, property damage, personal injury, violations of institutional, laboratory, hospital, ethical, human and animal treatment, privacy or other rules, regulations, laws, procedures or guidelines, liabilities and other losses or damages related in any way to the submission of work to JoVE, making of videos by JoVE, or publication in JoVE or elsewhere by JoVE. The Author shall be responsible for, and shall hold JoVE harmless from, damages caused by lack of sterilization, lack of cleanliness or by contamination due to the making of a video by JoVE its employees, agents or independent contractors. All sterilization, cleanliness or decontamination procedures shall be solely the responsibility of the Author and shall be undertaken at the Author's

expense. All indemnifications provided herein shall include JoVE's attorney's fees and costs related to said losses or damages. Such indemnification and holding harmless shall include such losses or damages incurred by, or in connection with, acts or omissions of JoVE, its employees, agents or independent contractors.

12. Fees. To cover the cost incurred for publication, JoVE must receive payment before production and publication of the Materials. Payment is due in 21 days of invoice. Should the Materials not be published due to an editorial or production decision, these funds will be returned to the Author. Withdrawal by the Author of any submitted Materials after final peer review approval will result in a US\$1,200 fee to cover pre-production expenses incurred by JoVE. If payment is not received by the completion of filming, production and publication of the Materials will be suspended until payment is received.

13. Transfer, Governing Law. This Agreement may be assigned by JoVE and shall inure to the benefits of any of JoVE's successors and assignees. This Agreement shall be governed and construed by the internal laws of the Commonwealth of Massachusetts without giving effect to any conflict of law provision thereunder. This Agreement may be executed in counterparts, each of which shall be deemed an original, but all of which together shall be deemed to be one and the same agreement. A signed copy of this Agreement delivered by facsimile, e-mail or other means of electronic transmission shall be deemed to have the same legal effect as delivery of an original signed copy of this Agreement.

A signed copy of this document must be sent with all new submissions. Only one Agreement required per submission.

CORRESPONDING AUTHOR:

Name:

Deutsch Mordechai

Department:

Physics Department


Institution:

Bar-Ilan University

Article Title:

Analysis of cancer cell invasion and anti-metastatic drug ...

Signature:



Date:

25.04.2018

Please submit a signed and dated copy of this license by one of the following three methods:

- 1) Upload a scanned copy of the document as a pdf on the JoVE submission site;
- 2) Fax the document to +1.866.381.2236;
- 3) Mail the document to JoVE / Attn: JoVE Editorial / 1 Alewife Center #200 / Cambridge, MA 02139

For questions, please email submissions@jove.com or call +1.617.945.9051



1 Alewife Center #200
Cambridge, MA 02140
tel. 617.945.9051
www.jove.com

ARTICLE AND VIDEO LICENSE AGREEMENT

Title of Article: Analysis of cancer cell invasion and anti-metastatic drug screening using hydrogel micro-chamber array (HAMCA)-based plates.
 Author(s): Bağcı-Hermes ÖRTE, Zeynep daşcı, Şaharhan Yana, Afrimzon Elend, Sabdev Marica, Hakuk Yaran, Bar-On Eizig Zehavit, Deutsch Mordechai

Item 1: The Author elects to have the Materials be made available (as described at <http://www.jove.com/publish>) via:

☒ Standard Access

☐ Open Access

Item 2: Please select one of the following items:

☒ The Author is **NOT** a United States government employee.

☐ The Author is a United States government employee and the Materials were prepared in the course of his or her duties as a United States government employee.

☐ The Author is a United States government employee but the Materials were NOT prepared in the course of his or her duties as a United States government employee.

ARTICLE AND VIDEO LICENSE AGREEMENT

1. **Defined Terms.** As used in this Article and Video License Agreement, the following terms shall have the following meanings: **"Agreement"** means this Article and Video License Agreement; **"Article"** means the article specified on the last page of this Agreement, including any associated materials such as texts, figures, tables, artwork, abstracts, or summaries contained therein; **"Author"** means the author who is a signatory to this Agreement; **"Collective Work"** means a work, such as a periodical issue, anthology or encyclopedia, in which the Materials in their entirety in unmodified form, along with a number of other contributions, constituting separate and independent works in themselves, are assembled into a collective whole; **"CRC License"** means the Creative Commons Attribution-Non Commercial-No Derivs 3.0 Unported Agreement, the terms and conditions of which can be found at: <http://creativecommons.org/licenses/by-nc-nd/3.0/legalcode>; **"Derivative Work"** means a work based upon the Materials or upon the Materials and other pre-existing works, such as a translation, musical arrangement, dramatization, fictionalization, motion picture version, sound recording, art reproduction, abridgment, condensation, or any other form in which the Materials may be recast, transformed, or adapted; **"Institution"** means the institution, listed on the last page of this Agreement, by which the Author was employed at the time of the creation of the Materials; **"JoVE"** means MyJoVE Corporation, a Massachusetts corporation and the publisher of The Journal of Visualized Experiments; **"Materials"** means the Article and / or the Video; **"Parties"** means the Author and JoVE; **"Video"** means any video(s) made by the Author, alone or in conjunction with any other parties, or by JoVE or its affiliates or agents, individually or in collaboration with the Author or any other parties, incorporating all or any portion

of the Article, and in which the Author may or may not appear.

2. **Background.** The Author, who is the author of the Article, in order to ensure the dissemination and protection of the Article, desires to have the JoVE publish the Article and create and transmit videos based on the Article. In furtherance of such goals, the Parties desire to memorialize in this Agreement the respective rights of each Party in and to the Article and the Video.

3. **Grant of Rights in Article.** In consideration of JoVE agreeing to publish the Article, the Author hereby grants to JoVE, subject to **Sections 4 and 7** below, the exclusive, royalty-free, perpetual (for the full term of copyright in the Article, including any extensions thereto) license (a) to publish, reproduce, distribute, display and store the Article in all forms, formats and media whether now known or hereafter developed (including without limitation in print, digital and electronic form) throughout the world, (b) to translate the Article into other languages, create adaptations, summaries or extracts of the Article or other Derivative Works (including, without limitation, the Video) or Collective Works based on all or any portion of the Article and exercise all of the rights set forth in (a) above in such translations, adaptations, summaries, extracts, Derivative Works or Collective Works and (c) to license others to do any or all of the above. The foregoing rights may be exercised in all media and formats, whether now known or hereafter devised, and include the right to make such modifications as are technically necessary to exercise the rights in other media and formats. If the "Open Access" box has been checked in **Item 1** above, JoVE and the Author hereby grant to the public all such rights in the Article as provided in, but subject to all limitations and requirements set forth in, the CRC License.

612542.6 For questions, please contact us at submissions@jove.com or +1.617.945.9051.

ARTICLE AND VIDEO LICENSE AGREEMENT

4. **Retention of Rights in Article.** Notwithstanding the exclusive license granted to JoVE in **Section 3** above, the Author shall, with respect to the Article, retain the non-exclusive right to use all or part of the Article for the non-commercial purpose of giving lectures, presentations or teaching classes, and to post a copy of the Article on the Institution's website or the Author's personal website, in each case provided that a link to the Article on the JoVE website is provided and notice of JoVE's copyright in the Article is included. All non-copyright intellectual property rights in and to the Article, such as patent rights, shall remain with the Author.

5. **Grant of Rights in Video – Standard Access.** This **Section 5** applies if the "Standard Access" box has been checked in **Item 1** above or if no box has been checked in **Item 1** above. In consideration of JoVE agreeing to produce, display or otherwise assist with the Video, the Author hereby acknowledges and agrees that, Subject to **Section 7** below, JoVE is and shall be the sole and exclusive owner of all rights of any nature, including, without limitation, all copyrights, in and to the Video. To the extent that, by law, the Author is deemed, now or at any time in the future, to have any rights of any nature in or to the Video, the Author hereby disclaims all such rights and transfers all such rights to JoVE.

6. **Grant of Rights in Video – Open Access.** This **Section 6** applies only if the "Open Access" box has been checked in **Item 1** above. In consideration of JoVE agreeing to produce, display or otherwise assist with the Video, the Author hereby grants to JoVE, subject to **Section 7** below, the exclusive, royalty-free, perpetual (for the full term of copyright in the Article, including any extensions thereto) license (a) to publish, reproduce, distribute, display and store the Video in all forms, formats and media whether now known or hereafter developed (including without limitation in print, digital and electronic form) throughout the world, (b) to translate the Video into other languages, create adaptations, summaries or extracts of the Video or other Derivative Works or Collective Works based on all or any portion of the Video and exercise all of the rights set forth in (a) above in such translations, adaptations, summaries, extracts, Derivative Works or Collective Works and (c) to license others to do any or all of the above. The foregoing rights may be exercised in all media and formats, whether now known or hereafter devised, and include the right to make such modifications as are technically necessary to exercise the rights in other media and formats. For any Video to which this **Section 6** is applicable, JoVE and the Author hereby grant to the public all such rights in the Video as provided in, but subject to all limitations and requirements set forth in, the CRC License.

7. **Government Employees.** If the Author is a United States government employee and the Article was prepared in the course of his or her duties as a United States government employee, as indicated in **Item 2** above, and any of the licenses or grants granted by the Author hereunder exceed the scope of the 17 U.S.C. 403, then the rights granted hereunder shall be limited to the maximum

rights permitted under such statute. In such case, all provisions contained herein that are not in conflict with such statute shall remain in full force and effect, and all provisions contained herein that do so conflict shall be deemed to be amended so as to provide to JoVE the maximum rights permissible within such statute.

8. **Protection of the Work.** The Author(s) authorize JoVE to take steps in the Author(s) name and on their behalf if JoVE believes some third party could be infringing or might infringe the copyright of either the Author's Article and/or Video.

9. **Likeness, Privacy, Personality.** The Author hereby grants JoVE the right to use the Author's name, voice, likeness, picture, photograph, image, biography and performance in any way, commercial or otherwise, in connection with the Materials and the sale, promotion and distribution thereof. The Author hereby waives any and all rights he or she may have, relating to his or her appearance in the Video or otherwise relating to the Materials, under all applicable privacy, likeness, personality or similar laws.

10. **Author Warranties.** The Author represents and warrants that the Article is original, that it has not been published, that the copyright interest is owned by the Author (or, if more than one author is listed at the beginning of this Agreement, by such authors collectively) and has not been assigned, licensed, or otherwise transferred to any other party. The Author represents and warrants that the author(s) listed at the top of this Agreement are the only authors of the Materials. If more than one author is listed at the top of this Agreement and if any such author has not entered into a separate Article and Video License Agreement with JoVE relating to the Materials, the Author represents and warrants that the Author has been authorized by each of the other such authors to execute this Agreement on his or her behalf and to bind him or her with respect to the terms of this Agreement as if each of them had been a party hereto as an Author. The Author warrants that the use, reproduction, distribution, public or private performance or display, and/or modification of all or any portion of the Materials does not and will not violate, infringe and/or misappropriate the patent, trademark, intellectual property or other rights of any third party. The Author represents and warrants that it has and will continue to comply with all government, institutional and other regulations, including, without limitation all institutional, laboratory, hospital, ethical, human and animal treatment, privacy, and all other rules, regulations, laws, procedures or guidelines, applicable to the Materials, and that all research involving human and animal subjects has been approved by the Author's relevant institutional review board.

11. **JoVE Discretion.** If the Author requests the assistance of JoVE in producing the Video in the Author's facility, the Author shall ensure that the presence of JoVE employees, agents or independent contractors is in accordance with the relevant regulations of the Author's institution. If more than one author is listed at the beginning of this Agreement, JoVE may, in its sole

ARTICLE AND VIDEO LICENSE AGREEMENT

discretion, elect not take any action with respect to the Article until such time as it has received complete, executed Article and Video License Agreements from each such author. JoVE reserves the right, in its absolute and sole discretion and without giving any reason therefore, to accept or decline any work submitted to JoVE. JoVE and its employees, agents and independent contractors shall have full, unfettered access to the facilities of the Author or of the Author's institution as necessary to make the Video, whether actually published or not. JoVE has sole discretion as to the method of making and publishing the Materials, including, without limitation, to all decisions regarding editing, lighting, filming, timing of publication, if any, length, quality, content and the like.

12. **Indemnification.** The Author agrees to indemnify JoVE and/or its successors and assigns from and against any and all claims, costs, and expenses, including attorney's fees, arising out of any breach of any warranty or other representations contained herein. The Author further agrees to indemnify and hold harmless JoVE from and against any and all claims, costs, and expenses, including attorney's fees, resulting from the breach by the Author of any representation or warranty contained herein or from allegations or instances of violation of intellectual property rights, damage to the Author's or the Author's institution's facilities, fraud, libel, defamation, research, equipment, experiments, property damage, personal injury, violations of institutional, laboratory, hospital, ethical, human and animal treatment, privacy or other rules, regulations, laws, procedures or guidelines, liabilities and other losses or damages related in any way to the submission of work to JoVE, making of videos by JoVE, or publication in JoVE or elsewhere by JoVE. The Author shall be responsible for, and shall hold JoVE harmless from, damages caused by lack of sterilization, lack of cleanliness or by contamination due to

the making of a video by JoVE its employees, agents or independent contractors. All sterilization, cleanliness or decontamination procedures shall be solely the responsibility of the Author and shall be undertaken at the Author's expense. All indemnifications provided herein shall include JoVE's attorney's fees and costs related to said losses or damages. Such indemnification and holding harmless shall include such losses or damages incurred by, or in connection with, acts or omissions of JoVE, its employees, agents or independent contractors.

13. **Fees.** To cover the cost incurred for publication, JoVE must receive payment before production and publication of the Materials. Payment is due in 21 days of invoice. Should the Materials not be published due to an editorial or production decision, these funds will be returned to the Author. Withdrawal by the Author of any submitted Materials after final peer review approval will result in a US\$1,200 fee to cover pre-production expenses incurred by JoVE. If payment is not received by the completion of filming, production and publication of the Materials will be suspended until payment is received.

14. **Transfer, Governing Law.** This Agreement may be assigned by JoVE and shall inure to the benefits of any of JoVE's successors and assignees. This Agreement shall be governed and construed by the internal laws of the Commonwealth of Massachusetts without giving effect to any conflict of law provision thereunder. This Agreement may be executed in counterparts, each of which shall be deemed an original, but all of which together shall be deemed to be one and the same agreement. A signed copy of this Agreement delivered by facsimile, e-mail or other means of electronic transmission shall be deemed to have the same legal effect as delivery of an original signed copy of this Agreement.

A signed copy of this document must be sent with all new submissions. Only one Agreement is required per submission.

CORRESPONDING AUTHOR

Name:

Mordechai Deutsch

Department:

Physics Department

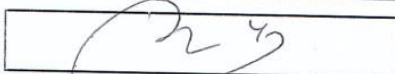
Institution:

Bar-Ilan University

Title:

Prof.

Signature:



Date:

17.7.2018

Please submit a **signed and dated** copy of this license by one of the following three methods:

1. Upload an electronic version on the JoVE submission site
2. Fax the document to +1.866.381.2236
3. Mail the document to JoVE / Attn: JoVE Editorial / 1 Alewife Center #200 / Cambridge, MA 02140

16.07.2018

Bing Wu, Ph.D.
Review Editor JoVE,

Dear Sir,

We wish to thank the Editor and the Reviewers for helping us to improve the quality and clarity of our manuscript. Reviewer comments are addressed below point-by-point as they appear in the review, and relevant changes have been incorporated into our revised manuscript. Answers to Reviewer comments appear after each comment in *italics*.

Editorial comments:

Changes to be made by the Author(s):

1. Please take this opportunity to thoroughly proofread the manuscript to ensure that there are no spelling or grammar issues. The JoVE editor will not copy-edit your manuscript and any errors in the submitted revision may be present in the published version.

The manuscript has been thoroughly proofread.

2. Figure 4: Please include a space between the number and unit of the scale bar (i.e., 500 μm).

This has been corrected, see new Figure 6.

3. Please rephrase the Long Abstract to more clearly state the goal of the protocol.

The Long Abstract has been revised; to more clearly state the goal of the protocol, see specifically, lines 78-80.

4. Please rephrase the Introduction to include a clear statement of the overall goal of this method.

The Introduction has been rephrased to include a clear statement of the goal, see lines 136-138.

5. Please define all abbreviations before use (DDW, RT, SD, etc.).

Abbreviations have all been defined at first appearance in the manuscript.

6. Please include a space between all numbers and their corresponding units: 15 mL, 37 $^{\circ}\text{C}$, 60 s; etc.

Spaces have been added between numbers and units throughout the manuscript.

7. 2.1: Please add more details to this step. This step does not have enough detail to replicate as currently written. For instance, what are the trypsinization reactions condition? What medium and what volume is used to wash?

Details have been added to this step, see lines 192-198.

8. There is a 2.75 page limit for filmable content. Please highlight 2.75 pages or less of the Protocol (including headings and spacing) that identifies the essential steps of the protocol for the video, i.e., the steps that should be visualized to tell the most cohesive story of the Protocol. Remember that non-highlighted Protocol steps will remain in the manuscript, and therefore will still be available to the reader.

The text for the video has been highlighted.

9. Please ensure that the highlighted steps form a cohesive narrative with a logical flow from one highlighted step to the next. Please highlight complete sentences (not parts of sentences). Please ensure that the highlighted part of the step includes at least one action that is written in imperative tense.

The highlighted steps mentioned above in comment 8 form a logical flow from one text to the next.

10. As we are a methods journal, please revise the Discussion to explicitly cover the following in detail in 3-6 paragraphs with citations:

- a) Critical steps within the protocol
- b) Any modifications and troubleshooting of the technique
- c) Any limitations of the technique
- d) The significance with respect to existing methods
- e) Any future applications of the technique

The Discussion section has been revised to include the above points. a) Critical steps within the protocol: embedding the spheroid in collagen, see lines 527-532. b) Any modifications and troubleshooting of the technique: re-seeding of cells when the occupancy is too low, see lines 532-534. c) Any limitations of the technique: the size and geometry of the HMCA described in the manuscript are designed to hold relatively small cell clusters (up to 150 μm). For analyzing cell migration from larger cell structures, designing a new array will be necessary, see lines 534-537. d) The significance with respect to existing methods: see lines 498-525 and 539-545. e) Any future applications of the technique: see lines 566-568.

11. References: Please do not abbreviate journal titles. Please include volume and issue numbers for all references.

References have been changed to meet the Reviewer's specifications - journal names are no longer abbreviated and volume and issue numbers are included.

12. Please remove trademark (™) and registered (®) symbols from the Table of Equipment and Materials.

Changes to Table of Equipment and Materials have been made as per Editor's above request.

Reviewers' comments:

Reviewer #1:

Summary of the key results:

Orit et al. report a micro-chamber array composed of agarose, collagen I, which can also include hyaluronan to form cancer spheroids to study invasion. Improved in vitro models to understand invasion are needed, as some in vivo models do not reproduce the physiology of human tumours. Using a PDMS stamp pyramid-shaped micro-wells are made in agarose that support spheroid formation in hydrogels prepared on collagen-based gels. Spheroid area and cell invasion are measured using confocal microscopy over several days. The methods describe quantification and analysis of these readouts using one ovarian and one breast cancer cell line with Matlab.

Revisions:

1. Line 63: Lower case hydrogel

This word has been removed from the short abstract, instead the acronym was added, see line 63.

2. Line 65: Remove space for extracellular

Space has been removed, see line 65.

3. Line 86: Define HMCA

HMCA has been defined in the title, see lines 1-2.

4. Line 90: Define HTS

HTS has been removed from the long abstract and defined at first appearance, on lines 125-126.

5. In the abstract, describe the cell types used and the use of Fisetin

Cell types and the use of Fisetin have been described in the revised long abstract as per Reviewer's request, see lines 85-89.

6. Line 95: Reference needed

Reference has been added and subsequent references re-numbered, see line 96 (reference 1).

7. Line 127: Reference needed

Reference has been added and subsequent references re-numbered, see line 129 (reference 14).

8. Protocol 1: Describe the dimensions of the pyramid microwells and the stamp need to produce the desired device

The dimensions of MCs and PDMS stamp (same dimensions but reverse structure) have been described in the revised manuscript, see lines 158-161. In addition, a new figure has been added, presenting a cross section of an MC with its dimensions, see new Figure 1.

9. Protocol 1.1: How is LMA sterilized?

LMA powder is dissolved in sterile PBS in a sterile bottle, while stirring and heating to 80 °C, making it semi-sterile. Thereafter, when LMA gelation has been achieved in the wells, the whole device is sterilized by UV light in a dedicated instrument. This step has been added to the protocol as section 1.5, see lines 182-183. The UV instrument has been added to the Table of Equipment and Materials, see line 14.

10. Protocol 3.2: How is sterility ensured using an ice bucket in the biosafety cabinet? Can something better be used?

The ice bucket is thoroughly cleaned with 70% ethanol and placed inside a biological hood for at least 10-20 minutes – enough time to be sterilized by the air flow.

11. What difference is there between 48 and 72 h spheroids?

Usually, 72-hour spheroids are larger than 48-hour spheroids. Incubation time is calibrated and determined according to the type of cell line and the size of spheroids used in the experiment. This parameter is kept constant throughout all the experiments of the same kind. For MCF7 cells, 48-hour spheroids were used, whereas for HeLa cells, 72-hour spheroids were used for invasion assay. This has been described on lines 206-207 in Protocol 2.4.

12. Line 222: After collagen mixture add (ECM gel) so it is clear what is being referred.

Protocol 6.3, (ECM mixture) has been added on line 260. This definition (ECM mixture) is more correct than (ECM gel) which was suggested by the Reviewer, due to the fact that the ECM (at this stage of the Protocol) has not yet become a gel.

13. Line 227: Switch pour to pipette

This has been changed as per Reviewer's suggestion; see line 265, Protocol 6.4.

14. Line 228: Is the plate sealed with parafilm when cooled at 4°C?

The plate is only covered with its lid without parafilm sealing. This has now been detailed on line 266, Protocol 6.4.

15. Line 239: Switch possibility to option

This has been switched as per Reviewer's request; see line 276, Protocol 7.2.

16. Line 256: Is spheroid center of mass accurate considering the geometry of the wells are pyramids? Perhaps consider geometric center as you are not accounting for the density of cells in the spheroid

The geometry of the micro well does not influence the shape of the spheroids. The cells are unable to attach to the hydrogel, thereby attaching to each other and forming a 3D floating object. The shape of the object is independent; see new Figure 5A&C, in which the images demonstrate properly the structure of the MC (truncated upside down square-shaped pyramid) and the independent structure of the spheroid (spherical shape). The center of mass at each time point is calculated by averaging the X and Y coordinate values of all pixels in the ROI which defines the spheroid.

17. Line 297: Report the correct number of significant digits based on detection accuracy

Based on detection accuracy of 10 measurements for one sample and calculation of standard error, the measurement error starts at the fifth digit after the decimal point for sectional area (mm²) and at the third digit after the decimal point for sphericity (a.u.). This has been corrected in the revised manuscript, see lines 340-343.

18. Line 304: Switch pour to pipette

This has been switched as per Reviewer's request, see line 358.

19. Line 318: Report the correct number of significant digits and units

The correct significant digits for the slopes are at the sixth digit after the decimal point based on error evaluation by the least squares regression method. Units of the slopes were added as well. This has been corrected in the revised manuscript, see lines 370-373.

20. Line 320: Describe what Fisetin targets

Fisetin activity and targets are now described and referenced; see lines 374-378 and reference 20.

21. Line 363: Switch X4 to 4X

This has been changed throughout the revised manuscript as per Reviewer's request, see lines: 274, 401, 427, 437, 444, 462 and 472.

22. Line 366: Switch 3 day old to day 3

This has been changed to 3-day throughout the revised manuscript, see lines: 323, 337, 344, 348, 355, 431, 443, 449-450, 459, 469 and 477.

23. Line 384: How are the linear regressions adjusted for each curve? What does this do? *Could you mean calculated?*

Linear regressions are adjusted using the automatic linear trendline option in excel software, this option uses the TREND function. TREND function fits a straight line (using the least squares method) to the arrays of known_y's and known_x's and returns new numbers in linear trend, matching the known data points. We calculated the slope of the linear trendline for each one of the spheroids and then executed the t-test on the slopes to determine if the two samples (collagen and collagen+HA) are significantly different. The trendline presented in the new Figure 5 has the mean slope of all the slopes in each sample.

24. Line 398: Define the acronym DETA

This has been defined at first appearance, see line 387.

24. Line 406: Switch X10 to 10X

This has been changed as per Reviewer's request, see lines: 233, 239, 274, 400, 452 and 478.

25. Figure 4B: Spheroids are missing from some micro wells how often does this occur?

In some of the experiments, while adding the ECM mixture to the spheroid array (or during other manipulations such as medium change), some of the spheroids

become dislocated from their MCs. This is the reason for the slow and gentle medium removal and ECM addition while leaning the tip on the hydrogel array edge (see Protocol steps 6.2 and 6.3.). Dislocation of 10-30% of the spheroids occurs in most experiments. However, in invasion protocol, which includes covering the spheroids with ECM, time 0 of the experiment is determined right after spheroids are embedded in ECM, hence missing spheroids are not included in the experiment. From that point on, spheroids will rarely dislocate.

26. Figure 4D: x- and y-axis are difficult to read

The figure has been replaced with a clearer one, as per Reviewer's request (see new Figure 6D).

27. Figure 5B: Some red areas of invading cells are not in micro wells are these artifacts of the software detection.

This is not an artifact. This happens in collective migration when the entire object is moving inside the ECM and changes its position relative to the MC.

Major revisions:

1. Long abstract has too much of a focus on introduction information and limited details about how this model can answer questions about understanding and developing drugs to prevent metastasis.

The long abstract has been revised accordingly, see lines 69-91.

2. This method does not address the limitations reported for in vivo breast or ovarian metastasis models.

We reported that in-vivo models for metastatic disease are expensive, have environments unlike the human microenvironment including ECM composition and non-tumor cells, and lack the ability to separate and control parameters. Indeed, the current in-vitro model is less expensive than most in-vivo animal models. Moreover, we have the ability with this method, to control parameters such as:

- 1. Spheroid size and composition, determined by the numbers and kinds of cells loaded into the array,*
- 2. ECM composition, by choosing ECM components adapted to human levels and to the type of cancer as well.*
- 3. Microenvironment cellular composition, by co-culturing tumor spheroids with cancer associated fibroblasts or immune cells in order to measure their influence on tumor invasion.*

However, in this work we did not exemplify all model options but rather focused on the principles.

3. The model is not described as a high-throughput system for performing drug screening in the method described. 6-well systems are not scalable to large arrays of drugs (100-1000's).

We have changed the text to read 'medium throughput', see lines 85 and 149-150. It is correct that a 6-well plate does not enable a large array of drugs. However, the sample size for each drug tested is very large (450 spheroids), which makes the measurement more accurate and lowers the number of repeats. This has been explained in the revised manuscript on lines 539-543. In reality, each macro well of a 6-well plate contains 4 times the number of spheroids than a 96-well plate.

4. Please detail why or cite the importance of inter-spheroid interaction for studying metastasis in drug screening.

The HMCA technology facilitates formation, treatment and continuous monitoring of individual multicellular structures derived from a distinct small number of cells confined to micro-chambers. Survival and function of individual cells/small cell clusters are enabled due to the fact that the cells/spheroids share the same space and medium and inter-spheroid interaction via soluble factors is possible. This explanation has been added to Discussion, see lines 522-525.

5. Protocol 5.3: The stiffness of hydrogels with collagen I and with hyaluronan are not defined in the method these should be reported.

Stiffness information for collagen and collagen with HA has been added to Discussion and referenced accordingly, see lines 557-560 and references 29-33.

6. Describe advantages of this model to other spheroid systems which also enable detection of cell viability?

This model enables detection of cell viability as well. A new Protocol section (step 3) and a new figure to exemplify this ability in the protocol have been added in the revised manuscript; see lines 209-226 in Protocol and lines 346-353 in Representative results. Also see new Figure 4 and Figure Legend lines 442-447. Detection of cell viability is conducted here after spheroid formation; in addition, it could also be performed after ECM addition and at the end of the invasion process as well. Optionally, other dyes detecting cell viability could be used; for details see lines 223-226.

7. The coefficient of variation described for these spheroids is quite high. Please discuss this in the context of other spheroid models relying on cell aggregation and how this variation exists between different micro-wells in other wells.

The CV described here (52.80%) is higher, compared to some other spheroid models. Castillo et al. (doi: 10.1038/srep28375) compares 3 different methods for spheroid formation and report a CV (sectional area) of 6-23%. The methods that Castillo et al. describe (hanging drops and low attachment 96 microplate) attain cell

distribution by pipetting cells directly to each well/drop. Sato et al. create embryoid bodies from pluripotent stem cells (doi.org/10.1038/srep31063) and report a CV (diameter of object) of 19-30%. Sato et al. attain cell distribution by loading cell suspension on top of the MC array and cells distribute by gravity into the MCs. Because spheroid size and homogeneity depend on initial number of cells per spheroid, the variation in cell distribution after cell loading derived from different methods should be considered. Therefore, comparing our CV to Sato et al. (same loading system) in the same parameter (diameter) will be more relevant. Considering spheroid diameter, we achieve a CV of 19-30% with average 24.52%, very similar to Sato et al. However, others (Lee et al. (DOI: 10.1063/1.3687409) who use loading by gravity as well), report lower CV values (sectional area) of 5.5-8.9%.

Our solution is to analyze spheroids at single-element resolution, which is more accurate than averaging the whole population, and reduces CV to 15.48% for sectional area and 7.45% for spheroid diameter. In some experiments, spheroids are analyzed by initial cell loading number. The CV between different wells for cell loading (24.37%) is similar to the one reported for hanging drops and low attachment plate (pipette cells directly to each well). The reply was briefly clarified in the revised manuscript as well; see lines 326-328.

8. While the authors describe quantitative methods to characterize cell invasion they do not discuss methods to characterize cell viability.

See our reply to comment #6. This work focused on invasion assay. Although viability screens using fluorescent probes are feasible in the HMCA plate, they were not thoroughly explored in this work, and thus, not discussed in detail in our manuscript.

9. Include a 3D reconstruction image of the spheroids so the geometry can be confirmed.

Confocal microscopy was not used in this work, but rather wide field microscopy. Geometry was previously checked by image acquisition at several focal planes and by histologic sections. See Supplementary Figure 1 in Reference #16 (doi.org/10.18632/oncotarget.21610). Other histological section data have been submitted but not yet published.

10. Graph the number of disengaged cells from more than five spheroids considering there are 450 micro chambers as reported in line 357.

A histogram which shows the distribution of cumulative value of disengaged cells has been added; see new Figure 8E and description on lines 416-419 in Results. The Figure Legend has been changed as well on lines 485-486.

11. There are many unsubstantiated claims in the discussion: Homogeneous spheroids

The text has been rephrased: "spheroid populations in which approximately 50% of the spheroids are comparable in size"; see line 518 and our reply to comment #7 as well.

Reliable analysis

The reliability of HMCA plate results depends on their compatibility with parameters and outcomes derived from other methods or methodologies. Such agreement was previously demonstrated for breast cancer spheroids (reference #16,) and in the current study for HeLa spheroid invasion capacity in the presence of MMW-HA.

Practical to screen thousands of drugs

This sentence relates to other methods available in the market and has been omitted from the revised manuscript in Discussion. With the HMCA technology, we can screen "thousands of spheroids per plate"; see lines 539-540.

Please include references: DOI: 10.3389/fonc.2017.00293

This reference (#8) has been added to the Introduction and subsequent references have been re-numbered; see line 121.

Reviewer #2:

Manuscript Summary:

Orit et al reported a cell culture system for analyzing the cancer cell invasion. The authors prepared microwell array structures using agarose hydrogel, seeded cells and formed spheroids, and finally embedded the spheroids in collagen gel. Quantitative analysis of cell migration was performed by analyzing the spheroid shape. The presented concept is interesting, but there are several points that need intense improvement and/or further clarification before publication in this journal.

Major Concerns:

(1) First of all, the authors did not properly explain the advantages of the current approach compared to previously reported methods. For example, microchannel-based invasion assays (Chung, Lab Chip. 2009, 269) and spheroid-based invasion assays (Evensen, PLoS One, 2013, e82811; Yamamoto, Plos One, 2014, e103502) have already been reported. More recently, hydrogel fiber-based assay was reported (Sugimoto, Lab Chip 2018, 1378). All these examples used hydrogels for analyzing 3D migration/invasion assay of cancer cells, but the authors did not cite these important literatures, and that is a critical weakness of this paper.

Advantages of the current approach over other previously reported hydrogel-based methods have been included in the Introduction and Discussion; see lines 115-

126, 498-525, citing above references; see lines: 123 reference #9, 124 reference #12, 504 reference #24 and 506 reference #25, as per Reviewer's suggestion.

(2) The authors did not distinguish the proliferation and migration abilities of the cancer cells, so it was unclear what the authors actually analyzed by using the presented system.

The most commonly used assay to quantitate invading cells is the Boyden chamber which uses ECM coated membrane. Cells that move through the ECM from one side of the membrane to the other are defined as invading cells. In the current work, we measure cells which leave the spheroid body and move through the surrounding ECM. This is considered an invasion process – otherwise the cells would continue to proliferate in/atop the spheroid body (as demonstrated in control experiments with spheroids lacking an ECM cover). Moreover, the possibility to stain cells with markers for proliferation and for invasion as well, in order to distinguish between the states was not in the scope of this work (although possible in the HMCA device). However, in kinetic BF images, cells were defined, which after drifting apart from the spheroid body became round and sometimes split into two round cells, thereafter changing again to regular/long shape and continuing their movement. There are works which report that invading cells switch between the states (DOI: 10.1158/0008-5472).

(3) It was unclear why the authors used two types of cancer cells for different experiments. The authors should clarify why there was a need to choose different cell types for different experiments.

Two kinds of cancer cells were used in order to exemplify the two kinds of invasion and their analysis. MCF7 cells commit collective invasion whereas HeLa cells commit single-cell invasion.

(4) The experimental procedures were not properly described. For example, the authors did not describe the concept of data processing, but just explained the software guides, and this is not appropriate. The software used for statistical analysis was not shown. It was unclear how many cells/colonies the authors observed for obtaining the data.

The concept of data processing was described as a Note in the Protocol section (right after step 7.5, see lines 284-297). Excel software was used for result processing and statistical analysis and this information has been added to the revised manuscript; see lines 306-307 and to the Table of Equipment and Materials, see line 22. Each figure legend indicates the number of spheroids that were observed and analyzed (n).

(5) The authors did not describe the reproducibility of the experimental results. Some of the descriptions in Results were not incomprehensible. For example, it is difficult to claim that the aggregates were "typically spherical".

All experiments were carried out at least twice, and each condition was duplicated in all experiments. Results have been re-checked and incomprehensible parts have been revised. The description "typically spherical" has been changed to 'more spherical' for accuracy; see line 338.

Minor Concerns:

(6) Abbreviations should be defined for the first time when they appear. Refs. 11 and 12 are identical. The authors should check entire manuscript once again if it is easily comprehensible.

Abbreviations have been defined at first use throughout the revised manuscript as per Reviewer's suggestion, and duplicate reference removed.

We thank you for your consideration.

Prof. Mordechai Deutsch
The Biophysical Interdisciplinary Jerome Schottenstein Center
for the Research and Technology of the Cellome,
Physics Department,
Bar Ilan University,
5290002, Ramat Gan, Israel
Tel: 03-5318349
Fax: 03-5342019
Email: motti.jsc@gmail.com

17.07.2018

To Bing Wu, Ph.D.
Review Editor JoVE,

Dear Sir,

We wish to thank the Editor for helping us to improve the quality and clarity of our manuscript. Answers to the Editor comments appear after each comment in *italics*.

Editorial comments:

The manuscript has been modified and the updated manuscript, **58359_R2.docx**, is attached and located in your Editorial Manager account. **Please use the updated version to make your revisions.**

1. Please take this opportunity to thoroughly proofread the manuscript to ensure that there are no spelling or grammar issues.

The manuscript has been thoroughly proofread. A few mistakes have been found and corrected.

2. Please do not highlight notes for filming.

Highlighted in notes have been removed.

3. Please use standard SI unit symbols and prefixes such as μL , mL, L, g, m, etc.

Standard units have been used throughout the manuscript.

4. Please use h, min, s for time units.

Time units have been corrected as per editor request. Except for the word 'day'.

5. Please highlight complete sentences (not parts of sentences) for filming.

Only complete sentences have been highlighted.

6. Please sign the new Author License Agreement, which is attached to this email. Please upload it to your Editorial Manager account when you submit your revision.

New Author License Agreement has been signed and uploaded.

We thank you for your consideration.

Prof. Mordechai Deutsch
The Biophysical Interdisciplinary Jerome Schottenstein Center
for the Research and Technology of the Cellome,

Physics Department,
Bar Ilan University,
5290002, Ramat Gan, Israel
Tel: 03-5318349
Fax: 03-5342019
Email: motti.jsc@gmail.com